

Hypotheses disambiguation in retrospective for robust perception in ambiguous environments

Ohad Shelly

Hypotheses disambiguation in retrospective for robust perception in ambiguous environments

Research Thesis

Submitted in partial fulfillment of the requirements
for the degree of Master of Science in Autonomous Systems and
Robotics

Ohad Shelly

Submitted to the Senate
of the Technion — Israel Institute of Technology
Adar 5782 Haifa February 2022

This research was carried out under the supervision of Associate Prof. Vadim Indelman, in the Technion Autonomous Systems Program.

Publications:

O. Shelly and V. Indelman. Hypotheses Disambiguation in Retrospective.

- IEEE Robotics and Automation Letters (RA-L), 2022.
IEEE Intl. Conf. on International Conference on Robotics and Automation (ICRA), 2022.

ACKNOWLEDGEMENTS

First, I would like to thank my advisor Associate Professor Vadim Indelman for all his guidance, help, support and patience through the years of my Master's studies. I honestly believe that he helped me in pushing my research abilities to the highest level, and that without his assistance through the years my research wouldn't have been where it is today.

I would also like to thank the people from Technion Autonomous Systems Program, especially to those from the ANPL lab for providing me constructive feedback throughout the years.

Finally, I would like to thank my family, My wife Noa and my two kids Omri and Alma for supporting me at achieving this final milestone.

The generous financial help of the Technion is gratefully acknowledged.

Contents

List of Figures

Abstract	1
Abbreviations and Notations	3
1 Introduction	5
1.1 Background	5
1.2 Motivation	6
1.3 Related Work	8
1.4 Contributions	9
1.5 Organization	9
2 Notation and problem formulation	11
2.1 Notations	11
2.2 Problem Formulation	12
3 Approach	13
3.1 Derivation of a General Formulation for $w_{m k}^i$	13
3.2 Single Step Update, $p = 1$	14
3.3 Multiple Steps Incremental Calculation of $w_{m m+p}^i$	15
3.3.1 $j = p - 1$	15
3.3.2 $j = p - 2$	16
3.3.3 General case	17
3.3.4 Final calculation of $\Psi_{m k}$	18
3.4 Re-Evaluation in Retrospective of a Specific Data Association Hypothesis	19
3.5 Enhanced Pruning of Hypotheses at Current Time	20
3.6 Computational Complexity Aspects and Algorithm	21
3.6.1 Computational Complexity	21
3.6.2 Algorithm	22
4 Results	23
4.1 Run-Time analysis and Entropy calculation	27

4.2	Enhanced Pruning of Hypotheses at Current Time	28
5	Conclusions and Future Work	29
5.1	Conclusions	29
5.2	Future work	29
6	Proof of Lemma 3.1	31
6.1	Base Case: $j = p - 2$	31
6.2	Induction assumption	33
6.3	Inductive step for $j = m + l$	34

List of Figures

1.1	Illustration for possible DA of two landmarks to a given measurement.	6
1.2	Motivation examples for weight re-evaluation, in the general case - (a) , as well for a specific simple setting - (b)	7
3.1	A simple setting for a specific DA probability re-evaluation.	19
3.2	A simple enhanced pruning example.	21
4.1	Robot's trajectory and initial estimation -"Prior", for both test cases in experiment section.	23
4.2	(a-c) Illustration of the robot's belief at key points on a <i>five steps</i> trajectory. (d) Original weight distribution at $k = 1$, VS the weight distribution given the information till current time. (e-f) Weight distribution at current time, with and without merging effect.	24
4.3	(a-c) Illustration of the robot's belief at key points on a <i>ten steps</i> trajectory. (d) Original weight distribution at $k = 1$, VS the weight distribution given the information till current time. (e-f) Weight distribution at current time, with and without merging effect.	26
4.4	Run-Time comparison between the Naive and the incremental approaches. Where figure (a) shows the Run-Time as a function of samples, and (b) shows the Run-Time as a function of the distance between current time from the re-evaluation point.	27
4.5	Histogram of the weight distribution at the re-evaluation point given information from future points in the robot's trajectory. Figure a shows the five steps trajectory case, and Figure b shows the ten steps trajectory case.	27
4.6	A simulation of a ten steps trajectory that shows the ability of enhanced pruning.	28

Abstract

As of today, most approaches that deal with the simultaneous localization and mapping (e.g. SLAM) of the robot's trajectory and surroundings assume that the data association, i.e. mapping between sensor measurements and the observed environment (e.g. landmarks), is given and perfect. Such an assumption can be very problematic in the real world, especially in highly ambiguous scenarios (for instance similar corridors), therefore Robust perception is a key required capability in robotics and AI - Artificial Intelligence. In such cases, one has to maintain multiple data association hypotheses which can be represented by a multi-modal belief. While the SLAM community has been addressing relaxing the data association from the front-end for some years now, current existing approaches are still computational expensive and address only certain aspects of the general problem.

In this work we contribute a framework that enables to update probabilities of externally-defined data association hypotheses from some past time with new information that has been accumulated until current time. In particular, we show appropriately updating probabilities of past hypotheses within this smoothing perspective potentially enables to disambiguate these hypotheses even when there is no full disambiguation of the mixture distribution at the current time. Further, we develop an incremental algorithm that re-uses hypotheses' weight calculations from previous steps, thereby reducing computational complexity. In addition we show how our approach can be used to enhance current-time hypotheses pruning, by discarding corresponding branches in the hypotheses tree. We demonstrate our approach in simulation, considering an extremely aliased environment setting.

Abbreviations and Notations

BSP	: Belief Space Planning
POMDP	: Partially Observable Markov Decision Process.
SLAM	: Simultaneous Localisation and Mapping.
iSAM	: Incremental Smoothing and Mapping.
GT-SAM	: Georgia Tech-Smoothing and Mapping.
GMM	: Gaussian mixture model.
x_k	: The robot's pose at time k
X_k	: The accumulative robot poses till at time k , denoted by $X_k = \{x_0, x_1, \dots, x_k\}$.
X_{k-p}	: past state vector for any valid value of $p \in [1..k-1]$.
u_k	: The robot's action at time k .
z_k	: Captured observation at time k .
l_i	: Landmark i representation where $i \in [1..L]$.
β_k	: Measurement z_k is associated to landmark (or object/scene) $l_{\beta_k=i}$, where $i \in [1..L]$.
H_k	: Accumulative vector of obtained measurements and actions till time k , via $\{z_{1:k}, u_{1:k-1}\}$.
H_k^-	: The propagated history vector till time k , via $\{z_{1:k-1}, u_{1:k-1}\}$.
$b[X_k]$: belief of state vector X_k , represented as a GMM.
$b^-[X_k]$: The propagated belief of state vector X_k .
$b^i[X_k]$: The i 'th hypothesis of the belief at time k .
γ_k	: An indicator of a given i hypothesis at time k .
	: The indicator is a vector of DA till time k , meaning $\gamma_k \doteq \{\beta_0, \beta_1, \dots, \beta_k\} = i$.
w_k^i	: The weight of the i 'th hypothesis at time k .
M_k	: The number of hypotheses at time k .
Σ_k	: covariance matrix of state vector X_k .
$\mathcal{H}(\cdot)$: differential entropy.

Chapter 1

Introduction

1.1 Background

Autonomous navigation in uncertain or unknown environments is essential in numerous applications in robotics, such as search and rescue, autonomous cars, indoor navigation, and surveillance. Once the robot operations take place in an unknown or uncertain environments, the navigation process also involves environment mapping. The corresponding problem, known as simultaneous localization and mapping (SLAM), has been extensively investigated [2–4] in the last two decades by the robotics and computer vision communities, where current approaches differ in various aspects, such as the inferred state, estimation method and sensors being used.

If we observe SLAM history as discussed by Durrant-Whyte and Bailey in [5] we see first approaches referring to extended Kalman filters, and maximum likelihood estimation. In particular, a seminal work by Davison et al [6] showed a first EKF-SLAM system that works online given a monocular imagery input. Yet, these early EKF-based approaches were not well-suited to large scale operation, as calculations are made in the covariance form.

Later period was the algorithmic phase, during which the research community focused on investigating and improving basic aspects in SLAM such as observability, convergence and consistency. A number of approaches that improved the efficiency and optimization of the problem are [7–11]. These works formulate SLAM as a maximum-a-posteriori estimation problem, and often use factor graphs to exploit the inherent sparsity of the underlying matrices and re-use calculations between consecutive time instances.

Computationally efficient online solvers that exploit the underlying inherent sparsity of the problem and re-use of calculations are readily available [12–14].

Traditional SLAM approaches include two parts, commonly known as the "front-end" and the "back-end". The latter maintains and updates a belief over robot past and current states (e.g. poses) and mapped environment given the available data at each time instant. This data can include any prior information, if exists, performed actions and captured sensor observations with the corresponding data association (DA). The latter is determined by the front-end process, and can be considered as associating observed scenes (e.g. in terms of landmarks) from current and previous time instances. A correct association between an observed landmark and a received

measurement is crucial for accurate inference.

A key common assumption is that the data association has been correctly determined by the front-end. Such an assumption, however, is less valid in presence of perceptual aliasing and ambiguity. Figure 1.1 for instance illustrates how from the uncertainty of our pose space from two different locations, one can observe two different landmarks from the scene space that will generate the same measurement in the observation space. An incorrect data association can lead to catastrophic results in inference/SLAM, e.g. the robot might deduce it is located in an incorrect similar-looking corridor, while assuming it is perfectly solved within planning can lead to sub-optimal actions, that could lead to collision and unsafe behavior, in general.

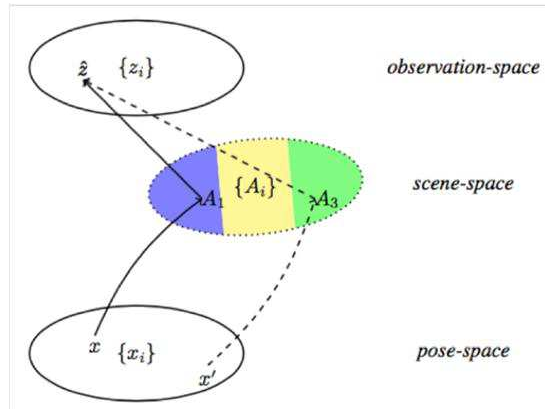


Figure 1.1: Two different landmark A_1 and A_3 from the scene space can be associated to the same measurement, via \hat{z} from two different poses, x and x' respectively. Figure taken from [15]

Relaxing the data association assumption would lead to robust perception approaches that are much required while operating in the real world [2], which typically exhibit some level of perceptual aliasing. Yet, this involves reasoning about DA as part of inference, and results in a set of hypotheses, where each one is built by a possible landmark association to the given measurement in hand. Such a formulation corresponds to a multi-modal belief, that can be represented, e.g. by a Gaussian mixture model (GMM) [16, 17].

1.2 Motivation

While robust inference approaches have been actively investigated in the last few years, till now existing approaches have dealt with relaxing the DA assumption while examining the state distribution at the *current* time instant. Moreover, except of [18], typically calculations are done from scratch for each time step, without calculation re-use.

In contrast, in this work we propose the notion of *hypotheses disambiguation in retrospective*, i.e. after more information has been collected. Our approach enables to re-evaluate the probability of externally-defined, key strategic hypotheses from a past time, given the information obtained up to the current time, while accounting for the data association hypotheses developed since that past time. A motivation can be seen in Fig. 1.2. The illustration in Fig 1.2a shows

a general case where we isolate an ambiguous event from some past time $k - p$, and wish to re-evaluate hypothesis i from that time given information obtained till time k .

We propose to utilize data that has been obtained since that time to update the posterior probabilities of these key past hypotheses. We envision such a capability and the general concept to be of interest in various contexts in robotics and beyond. For instance in Fig 1.2b we see a specific setting where one cant disambiguate any of the hypotheses, both at time $k - 1$ and at time k . In such a case examining the weight distribution at $k - 1$ given new obtained information might assist in the re-evaluation of a selected action, or in distinguishing the correct hypothesis by performing full disambiguation.

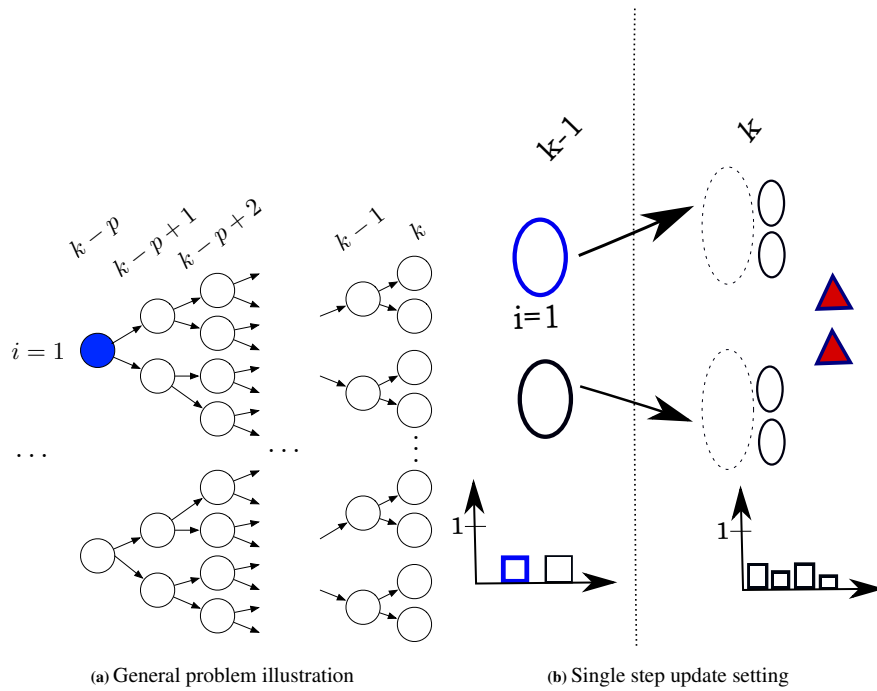


Figure 1.2: (a) In this work we aim to calculate the probability of externally-defined hypothesis from some past time $k - p$ given the information that has been obtained until current time k . In other words, we would like to calculate $w_{k-p|k}^i = \mathbb{P}(\gamma_{k-p} = i | H_k)$. The diagram illustrates, for simplicity, a branching factor of two, i.e. each hypothesis branches at the next time into two child hypotheses (e.g. due to obtained measurement with an ambiguous data association). For instance, we might be interested in calculating the weight $w_{k-p|k}^{i=1}$, which corresponds to probability of the hypothesis indicated by the blue node, given data until time k . (b) A toy example illustration of the general concept from (a), where $p = 1$, the prior belief is a Gaussian Mixture with two components, and upon performing an action the robot makes an observation z_k of one of two identical triangular landmarks. Due to ambiguous data association, the number of components in the posterior belief at time k is four. Posterior and propagated beliefs are denoted by solid and dashed lines, respectively. In this single step update scenario we wish to re-evaluate at time k the weight of hypothesis i from time $k - 1$, i.e. $w_{k-1|k}^i$, given the observation z_k .

1.3 Related Work

In the past years the research community has been actively investigating robust inference approaches to be resilient to false data association overlooked by front-end algorithms, i.e. by relaxing the assumption that the DA provided by front-end algorithms is outlier-free. An early work on DA is joint probability data association (JPDA) by Fortman et al. [19] which considers all possible DA options in the context of multi-target tracking. Some previous works refer to the case where a loop closure detection is reliable or false, by introducing a binary random variable for each loop closure candidate and solving inference via expectation-maximization [20,21]. Sunderhauf and Protzel [22] introduced the so called switchable constraints to detect faulty loop closures that lead to erroneous data association in back-end optimization. Other approaches include the so called switchable constraints, see e.g. [23]. Carlone et al. [24] address the problem from a different perspective, looking for a maximal coherent set among the given loop closure candidates. Olson and Agarwal [25] proposed a robust approach that uses max-mixture models. Wong et al. [26] presented a Dirichlet Process Mixture Model (DPMM) for data association in partially observed environments. More recently, optimization approaches robust to outliers have been investigated in works such as [27,28]. Finally, Fourie et al. [29] addressed computational aspects, aiming to update the GMM belief incrementally. One limitation of their approach, however, is that the association probabilities of a new measurement to different scenes/objects are assumed to have a uniform distribution, i.e. identical weights.

Another relevant work on active hypothesis disambiguation in the context of object detection and classification [30–33]. these approaches model a set of hypotheses for the landmarks pose and class in a given setting, and wish to retrieve a set of view points that will allow to perform full disambiguation, i.e. identifying the correct hypothesis. However this approaches assume the robot’s location is accurate. [34] addresses the issue of active SLAM while reducing the DA assumption, and wishes to find a set of actions to enable disambiguation and finding the correct hypothesis in the belief. Although we should note that the author assumes ambiguous setting only for initial belief, as well he assumes he can find a set of actions that leads to a full disambiguation.

A recent and more robust approach was shown by Pathak et al. [16] targets perceptual aliasing by explicitly reasoning about and probabilistically maintaining ambiguous DA hypotheses, in both inference and belief space planning. In contrast to many of the works mentioned above, it explicitly calculates the probability of different hypotheses, i.e. weights of GMM components, rather than assuming these to be identical. In addition it works in a more robust setting allowing ambiguous scenarios along the robot’s trajectory. Tchuiev et al. [17] extend the passive inference formulation from [16] by utilizing semantic information and viewpoint-dependent classifier models, as well as weight pruning to reduce the number of DA hypotheses.

1.4 Contributions

While the above-mentioned approaches address inference considering the (GMM) belief from the current time, we investigate a complimentary aspect, namely, utilizing current information to re-evaluate the probability of past, externally-specified, DA hypotheses. Specifically, building upon [16, 17] we develop a smoothing approach for updating the weights of past GMM beliefs, while properly accounting for the ambiguous data association hypotheses that have been acquired since then. Therefore, our main contributions are as follows:

1. We introduce the problem of hypotheses disambiguation in retrospective, which, to the best of our knowledge has not appeared thus far in literature.
2. We develop a probabilistic approach to update the probability of selected past hypotheses considering a smoothing formulation, while properly accounting for the ambiguous data association hypotheses that have been acquired since that time.
3. We derive a scheme for calculation re-use within this approach to reduce computational time.
4. We enhance hypotheses pruning also at *current* time, by leveraging the proposed concept of past hypotheses re-evaluation in retrospective and drawing a connection between hypotheses at current time and the corresponding ancestor hypotheses.
5. We evaluate our approach in simulation considering an extremely aliased environment comprising identical landmarks.

1.5 Organization

This thesis is organized as follows.

1. Chapter 2 introduces the belief in the GMM form, along with the basic setting this work is based on. In addition represents the formulation of the problem in hand.
2. Chapter 3 describes the mathematical development of our approach, along with complexity calculations for both approaches - the incremental one shown in this work, and the naive one, without calculation reuse.
3. Chapter 4 presents experimental results, and calculation comparison between both approaches.
4. Conclusions and possible future work are shown in Chapter 5.
5. For purpose of simplicity, the proof of the lemma 3.1 is moved into Appendix 6.

Chapter 2

Notation and problem formulation

2.1 Notations

Let x_k represent the robot current pose at time k , and denote by $X_k = \{x_0, x_1, \dots, x_k\}$ all robot poses until that time.

We define u_k and z_k to be, respectively, the robot's action and captured observation at time k . Further, we represent the environment by landmarks $L = \{l_i\}_{i=1}^{|L|}$, and assume they are static and known. We note that in case landmarks are uncertain, as in a typical SLAM setting, the observed landmarks up to time k would become part of the state X_k , and the formulation of our approach can be straightforwardly adjusted to such a setting. We should note, however, that such an extension will necessitate coping with the inherent curse of dimensionality, which is outside the scope.

Furthermore, the concept presented in this work is applicable also to other environment representations, such as grid-based localization, as long as one can formulate the corresponding data association hypotheses (see e.g. [16]).

Further, denote data association (DA) at time k by a discrete latent variable β_k , i.e. measurement z_k is associated to landmark (or object/scene) $l_{\beta_k=p}$, where $p \in [1, |L|]$. It is important to note that in the general case of obtaining a number of measurements in a single step, β_k would have been addressed to as a vector built from the landmarks associated to each measurement, as done in [17].

We use motion and observation models

$$x_k = g(x_{k-1}, u_{k-1}) + w \quad , \quad z_k = h(x_k, l_{\beta_k}) + v, \quad (2.1)$$

where $w \sim \mathcal{N}(\mu_w, \Sigma_w)$ and $v \sim \mathcal{N}(\mu_v, \Sigma_v)$. The process and measurement covariance matrices, Σ_w and Σ_v , as well as the functions $g(\cdot)$ and $h(\cdot)$ are assumed to be known.

Let history H_k represent all the robot's actions and received measurements till time k along with the set of known landmarks L , $H_k = \{z_{1:k}, u_{0:k-1}, L\}$. Similarly, denote by H_k^- history without the received measurement at time k , $H_k^- = \{z_{1:k-1}, u_{0:k-1}, L\}$. The probability density

function (pdf), the *belief*, at time k over X_k is then given by,

$$b[X_k] = \mathbb{P}(X_k | H_k). \quad (2.2)$$

Since we consider ambiguous scenarios, one cannot assume data association to be given and perfect. Similar to [16, 17], the number of hypotheses at time k , without yet considering pruning or merging, is given by all possible realizations of the sequence $\beta_{1:k} = \{\beta_1, \dots, \beta_k\}$. For convenience we denote $\gamma_k \triangleq \beta_{1:k}$, and consider at time k to have M_k hypotheses, i.e. $\gamma_k \in [1, M_k]$. Thus, the i th hypothesis, i.e. $\gamma_k = i$, corresponds to a specific sequence of $\beta_{1:k}$.

Hence, by marginalization of (2.2) over γ_k , and chain rule,

$$b[X_k] = \sum_{i=1}^{M_k} \underbrace{\mathbb{P}(\gamma_k = i | H_k)}_{w_k^i} \cdot \underbrace{\mathbb{P}(X_k | \gamma_k = i, H_k)}_{b^i[X_k]}, \quad (2.3)$$

where $b^i[X_k]$ and w_k^i represent, respectively, the conditional belief and the weight of the i th hypothesis at time k , and $\sum_{i=1}^{M_k} w_k^i = 1$. Finally, we denote the propagated belief as the belief conditioned on H_k^- instead of H_k , i.e. without considering the measurement at the current time, z_k . Similarly, a propagated belief for the i th hypothesis is defined as $b^{i-}[X_k] = \mathbb{P}(X_k | \gamma_k = i, H_k^-)$.

2.2 Problem Formulation

In this work we wish to re-evaluate, in retrospective, the probability of externally-specified hypothesis (or hypotheses) from some past time, i.e. given new information acquired since then. Specifically, we wish to re-evaluate a hypothesis weight for a given $\gamma_{k-p} = i$. Thus, our goal is to calculate

$$w_{k-p|k}^i \triangleq \mathbb{P}(\gamma_{k-p} = i | H_k), \quad (2.4)$$

where $1 \leq p < k$. In other words, in this work we investigate a smoothing perspective considering discrete random variables (data association hypotheses), which are, however, coupled with continuous random variables (e.g. robot poses).

Another variant of this problem is to re-evaluate the probability of some past association, β_{k-p} instead of a sequence of associations $\gamma_{k-p} \equiv \beta_{1:k-p}$. We consider this setting in Section 3.4.

We believe both problem variants can be of interest in different contexts: For example, considering specific realizations of γ_{k-p} may be useful in terms of localization, as each such realization corresponds to a posterior over X_k , see (2.3); This is in contrast to considering specific data association realizations from past time $k - p$, i.e. β_{k-p} , which can be of interest on its own. To shorten notations in the sequel, we denote $m \triangleq k - p$ and re-write (2.4) as $w_{m|k}^i \triangleq \mathbb{P}(\gamma_m = i | H_k)$.

Chapter 3

Approach

3.1 Derivation of a General Formulation for $w_{m|k}^i$

In this section we develop a general formulation for calculating (2.4). First, we perform Bayes rule considering the most recent measurement, z_k :

$$\mathbb{P}(\gamma_m = i | H_k) = \frac{\mathbb{P}(z_k | \gamma_m = i, H_k^-)}{\mathbb{P}(z_k | H_k^-)} \cdot \underbrace{\mathbb{P}(\gamma_m = i | H_{k-1})}_{w_{m|k-1}^i},$$

where we use, here and in the sequel, the fact $\mathbb{P}(\gamma_m = i | H_{k-1}, u_{k-1}) \equiv \mathbb{P}(\gamma_m = i | H_{k-1})$, i.e. the weights of a GMM are not impacted by the motion model.

Considering $w_{m|k-1}^i$, we now repeat the above process and perform Bayes rule once again, which yields,

$$\begin{aligned} \mathbb{P}(\gamma_m = i | H_k) &= \frac{\mathbb{P}(z_k | \gamma_m = i, H_k^-)}{\mathbb{P}(z_k | H_k^-)} \cdot \\ &\cdot \frac{\mathbb{P}(z_{k-1} | \gamma_m = i, H_{k-1}^-)}{\mathbb{P}(z_{k-1} | H_{k-1}^-)} \cdot \underbrace{\mathbb{P}(\gamma_m = i | H_{k-2})}_{w_{m|k-2}^i} \end{aligned} \quad (3.1)$$

It is not difficult to see that performing Bayes rule sequentially in a similar fashion yields the following formulation:

$$w_{m|k}^i = \left[\frac{\prod_{j=0}^{p-1} \mathbb{P}(z_{k-j} | \gamma_m = i, H_{k-j}^-)}{\underbrace{\prod_{j=0}^{p-1} \mathbb{P}(z_{k-j} | H_{k-j}^-)}_{\Psi_{m|k}}} \right] \cdot w_{m|m}^i \quad (3.2)$$

Here, $w_{m|m}^i$ is the weight of the i -th GMM component at time m , while $\Psi_{m|k}$ is the update factor that is based on the data obtained in the period $[m+1, k]$. Therefore, we need now to calculate this term in order to get $w_{m|k}^i$.

Since the denominator in (3.2) is not conditioned on $\gamma_m = i$, its explicit calculation can be

avoided. Instead, we first calculate the numerator,

$$\tilde{w}_{m|k}^i \triangleq \prod_{j=0}^{p-1} \mathbb{P}(z_{k-j} | \gamma_m = i, H_{k-j}^-) \cdot w_{m|m}^i, \quad (3.3)$$

for all $i \in [1, M_m]$, i.e. all hypotheses from time m , and then normalize as

$$w_{m|k}^i = \tilde{w}_{m|k}^i / \sum_{q=1}^{M_m} \tilde{w}_{m|k}^q. \quad (3.4)$$

Calculating (3.2) requires first computing the terms $\mathbb{P}(z_{k-j} | \gamma_m = i, H_{k-j}^-)$ for all $j \in [0, p-1]$.

In the next section we develop an approach to do so. Yet, naïvely, one would calculate each of the above terms from scratch. In contrast, in Section 3.3, we derive an incremental version, which re-uses calculations from previous steps.

3.2 Single Step Update, $p = 1$

We start with the simplest case of a single step update, i.e. $p = 1$ and $m = k - 1$, as illustrated in fig 1.2b. In this case, the un-normalized weight from (3.3) is given by

$$\tilde{w}_{m|k}^i = \mathbb{P}(z_k | \gamma_m = i, H_k^-) \cdot w_{m|m}^i. \quad (3.5)$$

To calculate $\mathbb{P}(z_k | \gamma_m = i, H_k^-)$ we marginalize over robot pose at time k and all the possible landmark associations β_k for the measurement z_k . Applying chain rule yields

$$\begin{aligned} \mathbb{P}(z_k | \gamma_m = i, H_k^-) &= \sum_{g=1}^{|\mathcal{L}|} \int_{x_k} \mathbb{P}(z_k | \beta_k = g, x_k, \gamma_m = i, H_k^-) \cdot \\ &\cdot \mathbb{P}(\beta_k = g | x_k, l_g) \cdot \underbrace{\mathbb{P}(x_k | \gamma_m = i, H_k^-)}_{b_m^i[x_k]} dx_k, \end{aligned} \quad (3.6)$$

where $\mathbb{P}(\beta_k = g | x_k, \gamma_m = i, H_k^-) \equiv \mathbb{P}(\beta_k = g | x_k, l_g)$ indicates the probability of observing the landmark l_g from robot pose x_k . Here, and throughout the paper, we use \square_m^i to indicate conditioning on $\gamma_m = i$.

We reiterate that, while we assume landmarks are known, in case landmarks are uncertain and part of the belief, we would need to also marginalize over them in (3.6).

Furthermore, for simplicity in this work we model $\mathbb{P}(\beta_k = g | x_k, l_g)$ as a uniform distribution with some finite support Ω_{l_g} (i.e. only for certain viewpoints, a given landmark is within sensor's field of view), and re-write (3.6) as

$$\mathbb{P}(z_k | \gamma_m = i, H_k^-) = \sum_{g=1}^{|\mathcal{L}|} \frac{1}{|\Omega_{l_g}|} \int_{x_k \in \Omega_{l_g}} \mathbb{P}(z_k | l_g, x_k) b_m^i[x_k] dx_k. \quad (3.7)$$

Since an analytical solution is not feasible, we resort to a sampling based approach and ap-

proximate (3.7) considering a set of $\{x_k^{n,i}\}_{n=1}^S$ sampled values from $b^i[x_k]$, with S denoting the number of samples:

$$\mathbb{P}(z_k | \gamma_m = i, H_k^-) \approx \frac{1}{S} \sum_{n=1}^S \sum_{g=1}^{|L|} \frac{1}{|\Omega_{l_g}|} \mathbb{P}(z_k | l_g, x_k^{n,i}) \mathbb{1}_{\Omega_{l_g}}(x_k^{n,i}), \quad (3.8)$$

where $\mathbb{1}_{\Omega_{l_g}}(x)$ is an indicator function, indicating if landmark l_g is within sensor's field of view from pose x .

Finally we calculate $w_{k-1|k}^i$ via normalization as in (3.4).

3.3 Multiple Steps Incremental Calculation of $w_{m|m+p}^i$

In the previous section we addressed the calculation of a single step update considering $p = 1$. In this section we consider the general case of $1 \leq p < k$, as illustrated in Fig. 1.2a, and develop a formulation to calculate the terms $\mathbb{P}(z_{k-j} | \gamma_m = i, H_{k-j}^-)$ from (3.2) for all $j \in [0, p - 1]$. While a naïve approach would calculate each of these terms from scratch, we develop an incremental version that allows to re-use calculations between different values of j .

We start by considering $j = p - 1$ and $j = p - 2$, and then discuss calculations for a general $j \in [0, p - 1]$.

3.3.1 $j = p - 1$

The corresponding term in (3.2) for $j = p - 1$ is $\mathbb{P}(z_{m+1} | \gamma_m = i, H_{m+1}^-)$. One can observe this is identical to the single step update case considered in Section 3.2, yet here we consider a single step from $m = k - p$. Therefore, following a similar process we generate a set of samples $\{x_{m+1}^{n,i}\}_{n=1}^S$ from the propagated belief $b_m^{i-}[x_{m+1}]$,

$$b_m^{i-}[x_{m+1}] \triangleq \mathbb{P}(x_{m+1} | H_{m+1}^-, \gamma_m = i), \quad (3.9)$$

and approximate $\mathbb{P}(z_{m+1} | \gamma_m = i, H_{m+1}^-)$ as

$$\frac{1}{S} \sum_{n=1}^S \sum_{g=1}^{|L|} \frac{1}{|\Omega_{l_g}|} \mathbb{P}(z_{m+1} | l_g, x_{m+1}^{n,i-}) \mathbb{1}_{\Omega_{l_g}}(x_{m+1}^{n,i-}), \quad (3.10)$$

which corresponds to (3.8). Note that for this first step, i.e. $j = p - 1$, $b_m^{i-}[x_{m+1}]$ is a Gaussian distribution. To shorten notations in the following sections, we denote

$$f(x, z) \triangleq \frac{1}{S} \sum_{g=1}^{|L|} \frac{1}{|\Omega_{l_g}|} \mathbb{P}(z | l_g, x) \mathbb{1}_{\Omega_{l_g}}(x). \quad (3.11)$$

Intuitively, $f(x, z)$ represents the probability of obtaining a given measurement z from robot pose x considering all possible data associations to the $|L|$ landmarks. Finally, substituting (3.11)

into (3.10) yields

$$\mathbb{P}(z_{m+1} | \gamma_m = i, H_{m+1}^-) \approx \sum_{n=1}^S f(x_{m+1}^{n,i}, z_{m+1}). \quad (3.12)$$

3.3.2 $j = p - 2$

We now consider calculation of the term $\mathbb{P}(z_{m+2} | \gamma_m = i, H_{m+2}^-)$ from (3.2). Similarly to (3.7), performing marginalization and chain rule, yields

$$\sum_{g=1}^{|\mathcal{L}|} \frac{1}{|\Omega_{l_g}|} \int_{x_{m+2} \in \Omega_{l_g}} \mathbb{P}(z_{m+2} | l_g, x_{m+2}) b_m^{i-}[x_{m+2}] dx_{m+2}, \quad (3.13)$$

where, as in (3.9), $b_m^{i-}[x_{m+2}] \triangleq \mathbb{P}(x_{m+2} | H_{m+2}^-, \gamma_m = i)$.

Performing chain and Bayes rules, marginalizing over x_{m+1} and data association hypotheses for z_{m+1} yields

$$\begin{aligned} b_m^{i-}[x_{m+2}] &= \frac{1}{\eta_{m+1}^i} \sum_{g=1}^{|\mathcal{L}|} \frac{1}{|\Omega_{l_g}|} \int_{x_{m+1} \in \Omega_{l_g}} \mathbb{P}(x_{m+2} | x_{m+1}, u_{m+1}) \\ &\cdot \mathbb{P}(z_{m+1} | l_g, x_{m+1}) b_m^{i-}[x_{m+1}] dx_{m+1}, \end{aligned} \quad (3.14)$$

where $\eta_{m+1}^i \triangleq \mathbb{P}(z_{m+1} | H_{m+2}^-, \gamma_m = i)$.

In practice, we approximate $b_m^{i-}[x_{m+2}]$ and η_{m+1}^i via sampling, considering S samples from $b_m^{i-}[x_{m+1}]$:

$$b_m^{i-}[x_{m+2}] \approx \sum_{n=1}^S \zeta_{m+1}^{n,i} \mathbb{P}(x_{m+2} | x_{m+1}^{n,i}, u_{m+1}), \quad (3.15)$$

and

$$\zeta_{m+1}^{n,i} \triangleq f(x_{m+1}^{n,i}, z_{m+1}) / \hat{\eta}_{m+1}^i, \quad (3.16)$$

with $\hat{\eta}_{m+1}^i \triangleq \sum_{n=1}^S f(x_{m+1}^{n,i}, z_{m+1})$, such that $\sum_{n=1}^S \zeta_{m+1}^{n,i} = 1$.

Note, the set of samples $\{x_{m+1}^{n,i}\}$ from $b_m^{i-}[x_{m+1}]$ was already obtained from section 3.3.1.

Further, observe that $b_m^{i-}[x_{m+2}]$ from (3.15) corresponds to a mixture belief over x_{m+2} , where each of the samples $x_{m+1}^{n,i}$ from the previous step is propagated via the transition model (2.1). Thus, in context of Sequential Monte Carlo (SMC), this corresponds to the bootstrap particle filter [35], i.e. where the proposal distribution is chosen to be transition model. Yet, here we also account for ambiguous data association aspects. Thus, as we consider in this work Gaussian models (2.1), $b_m^{i-}[x_{m+2}]$ is a GMM belief with S components, where $\zeta_{m+1}^{n,i}$ is the weight of the n th component.

Note that in (3.15) and (3.16) we have $f(x_{m+1}^{n,i}, z_{m+1})$. Instead of calculating it from scratch considering samples $x_{m+1}^{n,i}$ from the propagated belief $b_m^{i-}[x_{m+1}]$, our *key observation* is that it is

already available from the calculations for $j = p - 1$, see (3.12).

As before, we approximate the integral in (3.13) by generating a set $\{x_{m+2}^{n,i}\}_{n=1}^S$ of S samples from the GMM $b_m^{i-}[x_{m+2}]$ from (3.15), thus approximating $\mathbb{P}(z_{m+2} | \gamma_m = i, H_{m+2}^-)$ as

$$\frac{1}{S} \sum_{g=1}^{|\mathcal{L}|} \frac{1}{|\Omega_{l_g}|} \sum_{n=1}^S \mathbb{P}(z_{m+2} | l_g, x_{m+2}^{n,i}) \mathbb{1}_{\Omega_{l_g}}(x_{m+2}^{n,i}), \quad (3.17)$$

which, recalling the definition (3.11), can be finally written as

$$\mathbb{P}(z_{m+2} | \gamma_m = i, H_{m+2}^-) \approx \sum_{n=1}^S f(x_{m+2}^{n,i}, z_{m+2}) \triangleq \hat{\eta}_{m+2}^i. \quad (3.18)$$

3.3.3 General case

We are now in a position to calculate $\mathbb{P}(z_{m+j} | \gamma_m = i, H_{m+j}^-)$ for the general case. This is stated in the following Theorem.

Theorem 3.1. *The expression for $\mathbb{P}(z_{m+j} | \gamma_m = i, H_{m+j}^-)$ from (3.2) for any $j \in [2, p - 1]$ is given by,*

$$\mathbb{P}(z_{m+j} | \gamma_m = i, H_{m+j}^-) \approx \sum_{n=1}^S f(x_{m+j}^{n,i}, z_{m+j}) \triangleq \hat{\eta}_{m+j}^i. \quad (3.19)$$

A detailed proof via induction is given in 6.

Informally, as in (3.13), $\mathbb{P}(z_{m+j} | \gamma_m = i, H_{m+j}^-)$ can be written as

$$\sum_{g=1}^{|\mathcal{L}|} \frac{1}{|\Omega_{l_g}|} \int_{x_{m+j} \in \Omega_{l_g}} \mathbb{P}(z_{m+j} | l_g, x_{m+j}) b_m^{i-}[x_{m+j}] dx_{m+j}, \quad (3.20)$$

where $b_m^{i-}[x_{m+j}]$ is a GMM of S components,

$$b_m^{i-}[x_{m+j}] \triangleq \sum_{n=1}^S \zeta_{m+j-1}^{n,i} \mathbb{P}(x_{m+j} | x_{m+j-1}^{n,i}, u_{m+j-1}), \quad (3.21)$$

where, similar to (3.16),

$$\zeta_{m+j-1}^{n,i} \triangleq f(x_{m+j-1}^{n,i}, z_{m+j-1}) / \hat{\eta}_{m+j-1}^i, \quad (3.22)$$

with $\hat{\eta}_{m+j-1}^i \triangleq \sum_{n=1}^S f(x_{m+j-1}^{n,i}, z_{m+j-1})$.

The next step is to approximate the integral in (3.20) via sampling from the GMM $b_m^{i-}[x_{m+j}]$, which yields (3.19).

Similarly to Sec. 3.3.2, calculation re-use can be performed also for the general case considered here. To see that, note the set of samples $\{x_{m+j-1}^{n,i}\}_{n=1}^S$, as well as the corresponding values $f(x_{m+j-1}^{n,i}, z_{m+j-1})$ and η_{m+j-1}^i are already available to us from calculations performed for

the previous step, i.e. for $j - 1$, and thus can be conveniently re-used. In contrast, in the naive approach, one would have to re-sample the entire chain from scratch, i.e. starting with $m + 1$ and until $m + j - 1$.

3.3.4 Final calculation of $\Psi_{m|k}$

Based on (3.3), the un-normalized weight $\tilde{w}_{m|k}^i$ is

$$\tilde{w}_{m|k}^i \approx \prod_{j=0}^{p-1} \hat{\eta}_{k-j}^i \cdot w_{m|m}^i. \quad (3.23)$$

As mentioned in Section 3.1, calculating the normalized weight $w_{m|k}^i$ can be done via (3.4), which requires to first calculate $\tilde{w}_{m|k}^q$ for all hypotheses from time instant m , i.e. $\forall q \in [1, M_m]$.

3.4 Re-Evaluation in Retrospective of a Specific Data Association Hypothesis

In a similar manner, we can also consider a specific data association hypothesis $\beta_{k-p} = c$ from some past time $k - p$, with $c \in [1, |L|]$, rather than a sequence of data association hypotheses $\gamma_{k-p} \equiv \beta_{1:k-p} = i$ as done above. Note $i \in [1, M_{k-p}]$; without pruning $M_{k-p} = |L|^{k-p}$.

Indeed, by marginalizing over $\gamma_{k-p-1} \equiv \beta_{1:k-p-1}$ we get

$$\mathbb{P}(\beta_{k-p} = c | H_k) = \sum_{l=0}^{M_{k-p-1}} \mathbb{P}(\beta_{k-p} = c, \beta_{1:k-p-1} = l | H_k). \quad (3.24)$$

However, recall $\gamma_{k-p} \equiv \beta_{1:k-p}$, which can assume $M_{k-p} = M_{k-p-1} \cdot |L|$ values. Further, the probability for the i th realization of γ_{k-p} conditioned on H_k , i.e. $w_{k-p|k}^i$ with $i \in [1, M_{k-p}]$, is given by (3.2).

We now observe the index i designates a combination of some specific realization l of $\gamma_{k-p-1} \equiv \beta_{1:k-p-1}$ and some specific realization r of β_{k-p} . We shall denote these specific realizations for a given i as $i.l$ and $i.r$, respectively (standing for left and right).

Recall that w_{k-p}^i is available for any $i \in [1, M_{k-p}]$ from (3.2), see Section 3.3.4. Based on (3.24), we get

$$\mathbb{P}(\beta_{k-p} = c | H_k) = \sum_{i=1}^{M_{k-p}} w_{k-p|k}^i \mathbb{1}_{\{c\}}(i.r), \quad (3.25)$$

i.e. we sum only those realizations of γ_{k-p} that consider the c 'th data association from time $k - p$.

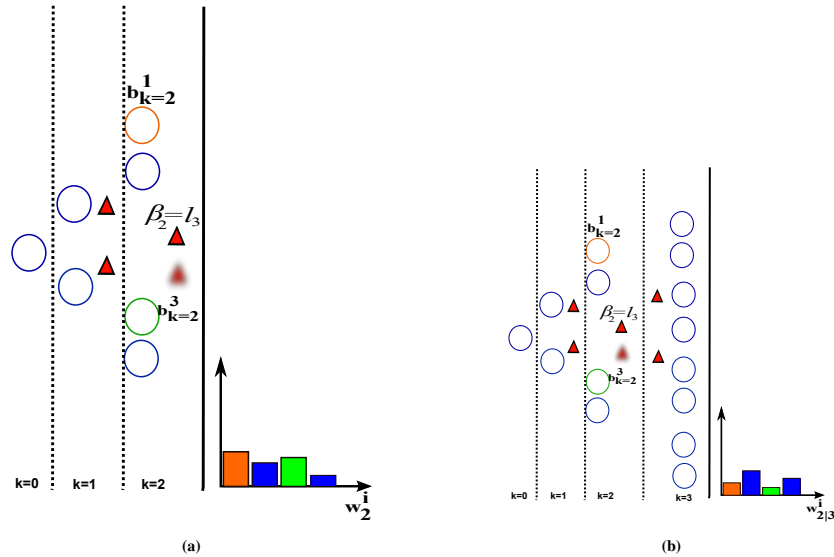


Figure 3.1: An example scenario on how new information can effect a specific DA evaluation. In **3.1a** the DA evaluation, via $\mathbb{P}(\beta_2 = l_3 | H_2)$ will be equal to the summation of the hypotheses weights that were generated by $\beta_2 = l_3$, meaning w_2^1 and w_2^3 . After performing re-evaluation as seen in **3.1b** the value of the weights is updated, and as a direct result our specific DA evaluation is updated as well, via $\mathbb{P}(\beta_2 = l_3 | H_3) = w_{2|3}^1 + w_{2|3}^3$.

The example above shows a simple case where at time $k = 2$ as shown in 3.1a the orange and green hypotheses are resulted from the same DA, via $\beta_2 = l_3$. Therefore the value of the probability for this specific DA to be the correct one, would be the summation of the weights for both of this hypotheses, meaning the green and orange weights. In 3.1b we obtain information at $k = 3$, therefore in a direct from, our updated weights due to re-evaluating the previous step weight distribution, would effect our ability to re-evaluate a specific DA as well.

3.5 Enhanced Pruning of Hypotheses at Current Time

Another immediate implication of our framework is the ability to enhance hypotheses pruning at current time. In detail, consider we re-evaluated in retrospective hypotheses $i \in [1, M_m]$ from past time $m = k - p$, i.e. $w_{k-p|k}^i$, as discussed in Section 3.3.4. Then, considering some user-specified pruning threshold th , for any $w_{k-p|k}^i < th$ we can prune also all its descendant hypotheses at time k .

More formally, considering the j th hypothesis at time k with $j \in [1, M_k]$, i.e. $\gamma_k \equiv \beta_{1:k} = j$, we again observe that index j designates a combination of some specific realization of $\beta_{1:k-p}$ and some specific realization of $\beta_{k-p+1:k}$. In a similar fashion to Section 3.4, we shall denote these realizations for a given j as $j.l$ and $j.r$, respectively (standing for left and right). Then, for any $w_{k-p|k}^i < th$ we can prune all hypotheses $j \in [1, M_k]$ from current time k that satisfy $j.l = i$. In other words, each hypothesis $j \in [1, M_k]$ is pruned if its ancestor hypothesis from time $k - p$, with index $j.l$ is below the pruning threshold th . The updated hypotheses' weights are therefore

$$\tilde{w}_k^j \doteq w_k^j \cdot \mathbb{1}_{\{j.l\}}(w_{k-p|k}^{j.l} > th). \quad (3.26)$$

In order to retrieve a valid GMM the weights should be re-normalized to sum to one, i.e. $w_k^j \doteq \tilde{w}_k^j / \sum_{j=1}^{M_k} \tilde{w}_k^j$, and the zero-weight (pruned) hypotheses discarded.

We note that, in general, a hypothesis j pruned this way may be above a pruning threshold, i.e. $w_k^j > th$, and thus would not be pruned without re-evaluating its ancestor hypothesis in retrospective, as suggested herein. We demonstrate this aspect in the results section.

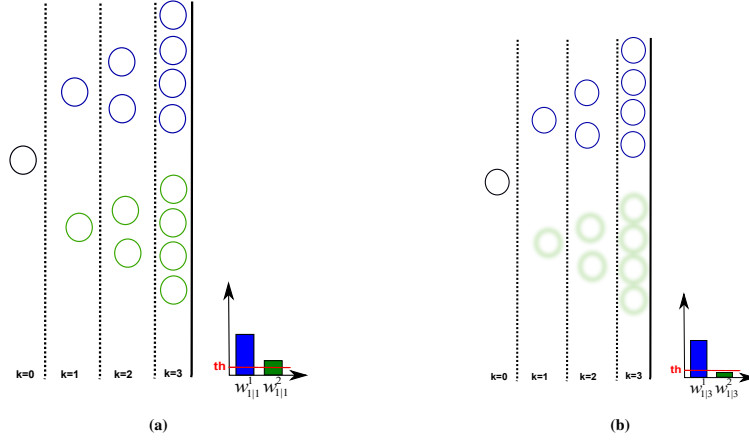


Figure 3.2: An example for enhanced pruning, where re-evaluation of a strategic point from the past, can result in pruning of all of the decedents of a given hypothesis. At **3.2a** Both hypotheses at $k = 1$ above threshold, therefore a full GMM tree is created till $k = 3$. Where in **3.2b** we see that $w_{1|3}^2$ is below pruning threshold, therefore all descendants of b_2^2 can be pruned.

In the example above we see a case where at $k = 1$ none of weights are pruned given the information till that time, this resulted in a full GMM spanning tree created till $k = 3$, as seen in 3.2a. Yet on the other hand, when we perform re-evaluation, we notice $w_{1|3}^2$ is below pruning threshold, therefore all of its **descents** can be pruned as well, and specifically the once at current time, via $k = 3$, as seen in 3.2b. By that our updated GMM at current time holds four hypotheses instead of eights, with updated values for there weights, as a result of normalization.

3.6 Computational Complexity Aspects and Algorithm

3.6.1 Computational Complexity

Calculating $w_{m|k}^i$ involves computation of the unweighted weights $\tilde{w}_{m|k}^q$, using (3.23), for *each* of the M_m hypotheses from time instant m , and then normalization via (3.4). For each given $q \in [1, M_m]$, following (3.23), this involves calculating $\hat{\eta}_{k-j}^q$ for all $j \in [0, p - 1]$, i.e. from $\hat{\eta}_{k-p+1}^q \equiv \hat{\eta}_{m+1}^q$ until $\hat{\eta}_k^q \equiv \hat{\eta}_{m+p}^q$.

In the naïve approach, such calculations are performed from scratch for each $\hat{\eta}_{k-j}^q$. In other words, as described in previous sections, this involves sequentially sampling the beliefs from time instances k until $k - j$, for *each* $j \in [0, p - 1]$. Assuming the same number of samples is taken at each time, for a given j , with $j \in [0, p - 1]$, this operation involves generating S samples j times. Hence, evaluating (3.23) is

$$\underbrace{S}_{j=p-1} + \underbrace{2 \cdot S}_{j=p-2} + \dots + \underbrace{p \cdot S}_{j=0} = \frac{(1+p) \cdot p}{2} \cdot S \in O(p^2 S).$$

As this evaluation has to be performed M_m times, the overall complexity of the naïve approach is $O(p^2 S M_m)$.

In contrast, our approach uses calculations in a recursive form, therefore we only need N

samples for every calculation of η_{k-j}^q . Thus, evaluating (3.23) is

$$\underbrace{S}_{j=p-1} + \underbrace{S}_{j=p-2} + \dots + \underbrace{S}_{j=0} = p \cdot S \in \mathcal{O}(p \cdot S),$$

and the corresponding overall complexity of our approach is $\mathcal{O}(pS M_m)$, i.e. one order of magnitude smaller in p than the naïve approach.

3.6.2 Algorithm

Algs. 3.1 and 3.2 summarize our approach from Section 3.3.

Algorithm 3.1 $w_{m|k}^i$ calculation

- 1: **Inputs:**
 - 2: H_k : History at time k
 - 3: $b[X_m]$: GMM belief at time $m = k - p$
 - 4: i : hypothesis index from time $m = k - p$
 - 5:
 - 6: **for** $q=1:M_m$ **do**
 - 7: Calculate $\tilde{w}_{m|k}^q$ using Alg. 3.2.
 - 8: **end for**
 - 9: **▷** Normalization via (3.4)
 - 10: $w_{m|k}^i = \tilde{w}_{m|k}^i / \sum_{q=1}^{M_m} \tilde{w}_{m|k}^q$
 - 11: **return** $w_{m|k}^i$
-

Algorithm 3.2 $\tilde{w}_{m|k}^i$ calculation with computation re-use

- Inputs:**
 - 2: H_k : History at time k
 - $b[X_m]$: GMM belief at time $m = k - p$
 - 4: q : hypothesis index from time $m = k - p$
 - 6: **for** $j = 1 : p$ **do**
 - if** $j = 1$ **then**
 - 8: Sample set $\{x_{m+1}^{n,q}\}_{n=1}^S$ from $b_m^{q-}[x_{m+1}]$, see Sec. 3.3.1
 - else**
 - 10: **Reuse** $\{\zeta_{m+j-1}^{n,q}\}_{n=1}^S$ to form a GMM belief $b_m^{q-}[x_{m+j}]$ from (3.21)
 - Sample set $\{x_{m+j}^{n,q}\}_{n=1}^S$ from $b_m^{q-}[x_{m+j}]$
 - 12: **end if**
 - Calculate $\hat{\eta}_{m+j}^q$ using samples $\{x_{m+j}^{n,q}\}_{n=1}^S$ as shown in (3.19).
 - 14: Calculate weights $\{\zeta_{m+j}^{n,q}\}_{n=1}^S$ via (3.22) for sample set $\{x_{m+j}^{n,q}\}_{n=1}^S$
 - end for**
 - 16: Calculate and return $\tilde{w}_{m|k}^q$ via (3.23):
-

Chapter 4

Results

In this section we examine our proposed algorithm in simulation considering an extremely perceptually aliased environment comprising $|L| = 8$ *identical* spatially scattered static known landmarks. Our simulations are based on the GTSAM library [13] with a Matlab wrapper.

The robot acquires relative pose observations to landmarks during its motion, yet the data association is not assumed to be externally provided, i.e. it is *unknown* which landmark generated each observation. Two scenarios of 5 and 10 time steps and differently scattered landmarks are considered, as shown in Figs. 4.1a and 4.1b. In both cases, the robot starts with a uni-modal Gaussian prior belief on its initial location, $b[X_0]$ and performs a pre-defined trajectory.

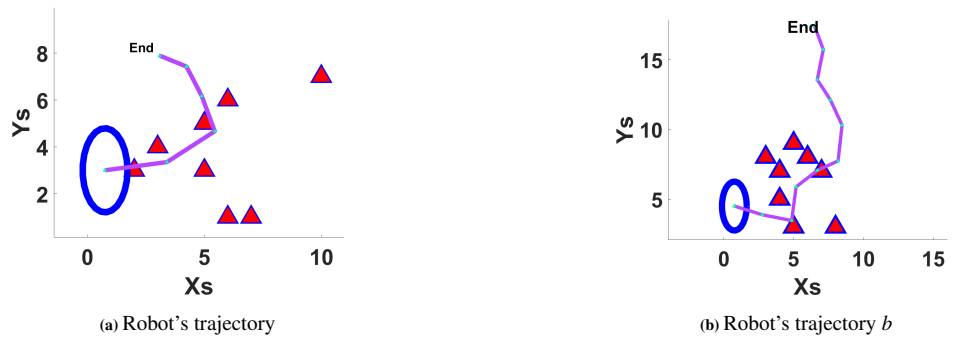


Figure 4.1: Ground truth trajectory for both for five steps as shown in *a*, and ten steps as shown in *b*. Both figures also show the initial prior belief, and ambiguous landmark setting.

We use a diagonal process covariance matrix Σ_w with standard deviation (std) of position of 0.5 meters and std of orientation of *mrad*. The measurement covariance matrix Σ_v is also diagonal with position std of 0.48 meters and orientation std of $0.87 \cdot 10^{-2}$ radians.

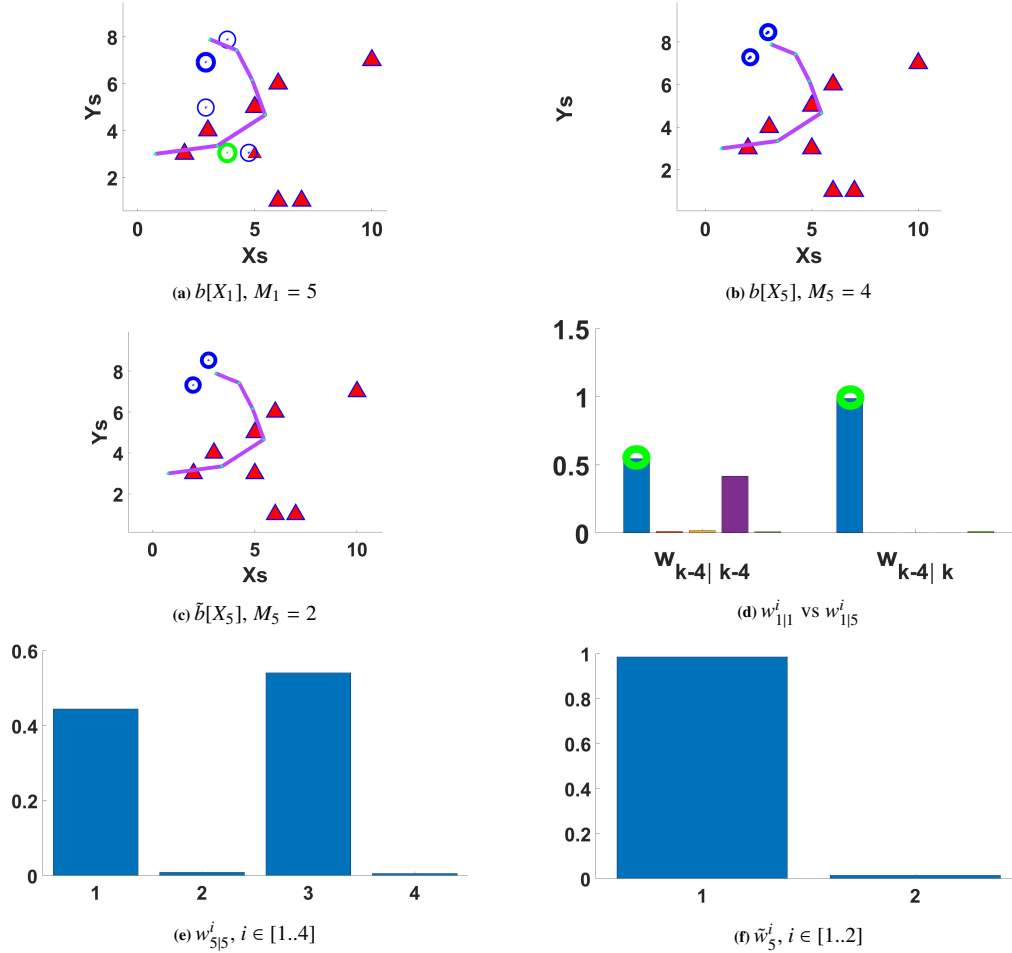


Figure 4.2:]

First scenario: **(a)** $b[X_{k=1}]$ is a GMM with five components. We choose this point as our **”re-evaluation”** point, where we test our algorithm. The hypothesis marked in green, states the correct hypothesis generated from the landmark associated to the given measurement. Notice that the **bolder** lines correspond to a higher weight of the hypothesis. **(b)** GMM belief at $k = 5$; we should note that the number of components doesn’t increase from the ”re-evaluation” point as a result of pruning. **(c)** The belief at $k = 5$ after merging, which reduces the number of hypotheses to $M_5 = 2$. **(d)** The calculated weight distribution at time $k = 1$ given the gathered information up to time $k = 1$ (see **(b)**), and given information up to time $k = 5$. The green circle marks the weight of the correct hypothesis as shown in **(b)**. **(e)** The current weight distribution of $b[X_5]$ as shown in **(b)**, via $w_{k=5|k=5}^i$, where $i \in [1..M_5]$ and $M_5 = 4$. **(f)** Current weight distribution after merging, i.e. $\tilde{b}[X_5]$, where $M_5 = 2$.

Figs. 4.2 and 4.3 show the results for both scenarios. At each time step k , following [16, 17], we update the belief from the previous time with the performed action and acquired observation with unknown data association, producing $b[X_k]$ from (2.3). For each case, we show in Figs. 4.2(a)-(b) and Figs. 4.3(a)-(b) the corresponding posterior GMM belief, shown in blue at specific time instances of interest.

Theoretically, the number of GMM components, grows exponentially according to the recursion $M_k = M_{k-1} \cdot |L|$. However, we prune components with negligible weights and show only the remaining components. Further, similarly to [16, 17], we occasionally merge sufficiently similar components, as shown in Fig 4.3c and 4.2c. We use the notation $\tilde{\square}$ to denote the belief and components weights after merging.

Given the above, in both scenarios we consider the i th data association hypothesis from time instant 1, and execute Alg. 3.1 to re-evaluate its probability in retrospective, i.e. given current time is k we calculate $w_{1|k}^i$.

For each step in our weight update we take a set of $S = 1000$ samples from the GMM created via (3.21). In our current implementation, samples are taken globally from the entire GMM, where the number of samples per each component is determined according to the GMM weights distribution.

The results for the first and second scenarios are shown, respectively, in Figs. 4.2d and 4.3d. In both cases we can see that at $k = 1$ we lack the ability to disambiguate between the hypotheses, however when using the information up to time $k = 5$ and $k = 10$ respectively, we can perform full disambiguation according to the updated weight distribution, via $w_{1|k}$ where $k \in [5, 10]$. In addition in the second test case shown in Fig. 4.3 we see that even after new information has been acquired along the trajectory, we still have an ambiguous setting with or without the merging effect: the corresponding weight distribution of the current belief includes several non-negligible hypotheses at $k = 10$, as shown in Figs. 4.3e and 4.3f. This is in contrast to the first scenario that after merging shows a single none negligible weight as shown in Fig. 4.2f. Nevertheless, as shown in Figs. 4.2d and 4.3d, our approach to update the weights in retrospective utilizing the information acquired until time k leads to more informative weight distributions. In particular, in both considered scenarios one of the hypotheses' value becomes substantially higher than the rest.

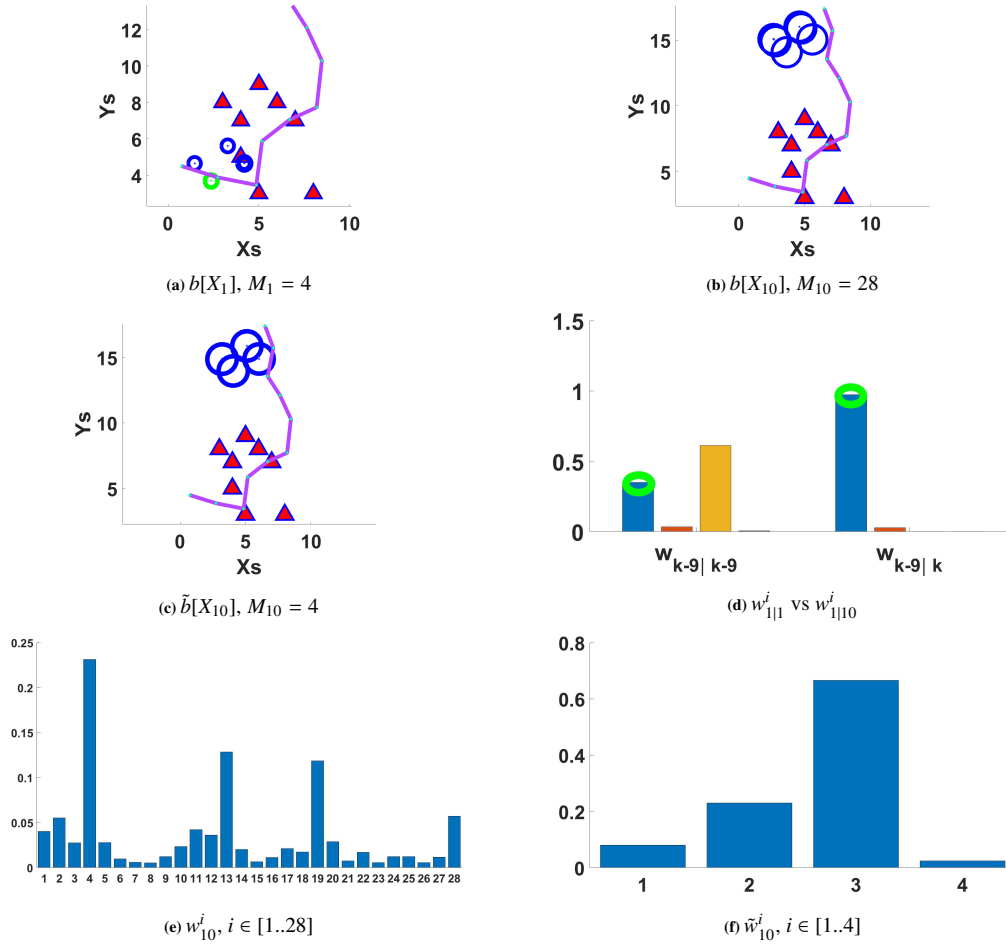


Figure 4.3:]

Second scenario: **(a)** The belief at $k = 1$, our **re-evaluation** point, is a GMM with four components. The hypothesis marked in green, states the correct hypothesis generated from the landmark associated to the given measurement. **(b)** The updated belief at current time, $k = 10$. Due to the ambiguity of the environment, the number of hypotheses increased from $M_1 = 4$ to $M_{10} = 28$ given pruning. **(c)** The belief at $k = 10$ with the merging effect, reduces the number of hypotheses to $M_{10} = 4$. **(d)** The calculated weight distribution at time $k = 1$ given the gathered information up to time $k = 1$, and given information up to time $k = 10$. The green circle marks the weight of the correct hypothesis as shown in 4.3a. **(e)** The current weight distribution of $b[X_{10}]$, i.e. $w_{k=10|k=10}^i$, where $M_{10} = 28$. **(f)** Current weight distribution after merging, $\tilde{b}[X_{10}]$, where $M_{10} = 4$.

4.1 Run-Time analysis and Entropy calculation

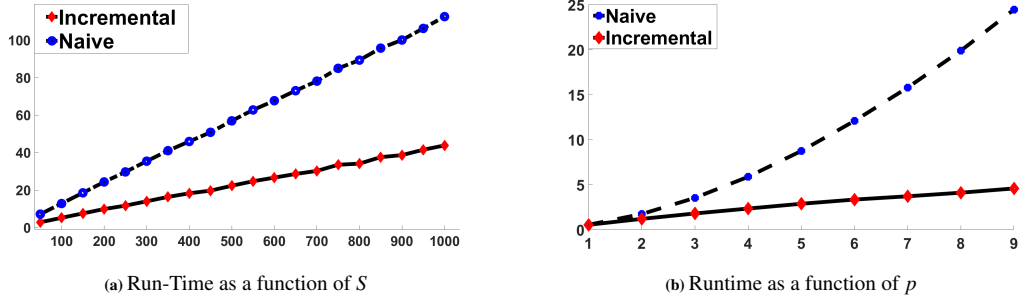


Figure 4.4: (a) Run-Time in seconds of $w_{k-4|k}^i$ calculation vs. number of samples S . The calculation was performed for both the naïve and the proposed incremental approach. (b) Run-Time in seconds of $w_{k-p|k}^i$ calculation vs. p for the naïve and the proposed incremental approach.

We also report runtime for both the naïve and our incremental approach. For the first scenario we calculated runtime as a function of number of samples $S \in [50, 1000]$, where the result per a number of samples is the statistical average of 20 runs. As shown in Fig. 4.4a the naïve approach calculation grows in a higher rate than the incremental. For the second scenario, as shown in Fig. 4.4b, we calculated the runtime as a function of the parameter p , see e.g. (2.4), where for this analysis the number of samples was fixed at 100. The runtime of the naïve approach shows a growth at a rate of p^2 , while the incremental one increases in a linear rate of p , which is in correlation to our calculation in Section 3.6.1.

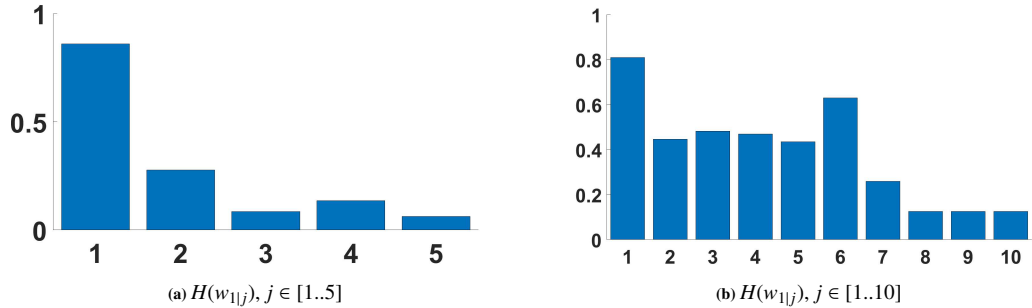


Figure 4.5: a The histogram of weight distribution at $k = 1$ given information at different time points for the five steps trajectory case, via $H(w_{1|j})$ where $j \in [1..5]$, and $i \in [1..M_1]$. b The histogram of weight distribution at $k = 1$ given information at different time points for the ten steps trajectory case, via $H(w_{1|j})$ where $j \in [1..10]$, and $i \in [1..M_1]$.

In addition Figs. 4.5a and 4.5b show the entropy of the weight distribution at the "re-evaluation" point given information at different time instances, i.e. $H(W_{1|j}) = -\sum_{i=1}^{M_1} w_{1|j}^i \cdot \log(w_{1|j}^i)$ where $j \in [1, k]$. Both test cases show that as we use more information at the "re-evaluation" point, the level of uncertainty can reduce, although we should mention that this is not guaranteed, since it is conditioned on the landmarks setting, and the randomized samples values.

4.2 Enhanced Pruning of Hypotheses at Current Time

In a similar simulation setting comprising eight identical landmarks and a trajectory of 10 time steps we examined the enhanced pruning of hypotheses at *current* time after re-evaluation in retrospective of past hypotheses (at $k = 1$), as discussed in Section 3.5. Results are shown in Fig. 4.6.

Fig. 4.6a shows that at time $k = 1$ there are two un-pruned hypotheses, i.e. whose weights are higher value than the pruning threshold $th = 0.005$. After we perform re-evaluation, hypotheses $w_{1|10}^1$ was pruned, and we remain with a single hypotheses $w_{2|10}^1$ marked in orange. As discussed in Section 3.5, all the descendant hypotheses of $w_{1|10}^1$ can now be discarded. These hypotheses are shown in blue color in the GMM "hypotheses tree" in Fig. 4.6d. More in detail, Fig. 4.6b shows the weights of the original GMM belief at $k = 10$, with $M_{10} = 14$ components: 4 descendant hypotheses of w_1^1 and 10 of w_2^1 , marked in blue and orange, respectively. Note all components are *above* the pruning threshold th . Fig. 4.6c shows the reduced GMM after pruning all the blue hypotheses (descendants of $w_{1|10}^1$) and re-normalizing the weights. Thus, leveraging the proposed concept the number of components reduces to 10.

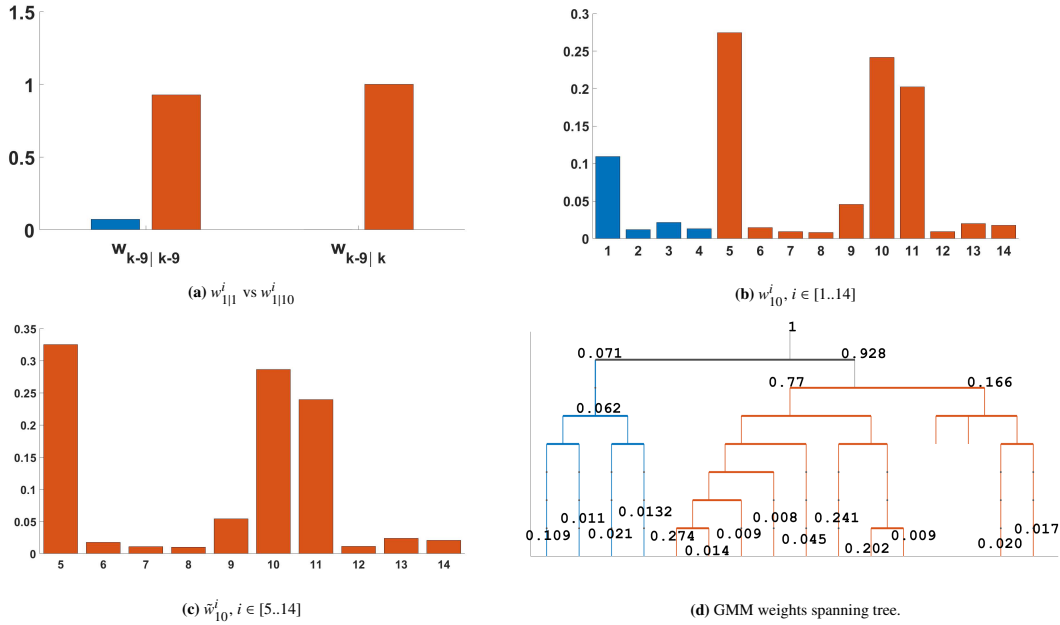


Figure 4.6: (a) The calculated weight distribution at time $k = 1$ given the gathered information up to time $k = 1$, and given information up to time $k = 10$. (b) The weight distribution at $k = 10$. The descendants of w_1^1 and w_2^1 are marked in blue and orange, respectively. In total we have $M_{10} = 14$ hypotheses (GMM components). (c) The updated weight distribution at $k = 10$, where all descendants of w_1^1 have been discarded after re-evaluation of the weights at $k = 1$. The number of hypotheses reduces to 10. (d) The entire hypothesis tree describing the evolution of hypotheses (GMM belief components) from the initial time and until the current time $k = 10$. Blue and orange colors represent descendant hypotheses of w_1^1 and w_2^1 , respectively.

Chapter 5

Conclusions and Future Work

5.1 Conclusions

We presented an approach to update probabilities of externally-specified hypotheses from some past time with information obtained since then and until the current time. Our approach is particularly of interest in the context of robust perception and autonomous navigation in ambiguous and perceptually aliased scenarios, which necessitate reasoning about data association hypotheses and thus to maintain mixture distributions such as GMM. In addition we developed an incremental form for calculation re-use, as opposed to a naïve approach that performs re-calculation in each step. Another direct consequence of our approach is enhanced pruning of hypotheses at current time, leveraging the updated weights of corresponding ancestor hypotheses given information thus far. Our simulation shows that re-evaluation of a past time in a highly aliased setting can assist with hypotheses disambiguation both in past and current time, and with our ability to discard an entire branch(es) from the GMM hypothesis tree.

5.2 Future work

Possible directions for future work can be,

1. Study the performance of our approach in different real world settings, and see how it effects the calculated run-time of our algorithm in appose to the naïve approach.
2. Add uncertainty to our scattered landmark in a given setting, and explore how this effects both the formulation of our solution, as well to the aspect of calculation time.
3. In our work we have explored the effect of current time information on a past strategic point in the robot's trajectory. However our work deals with the correlation of the full GMM spanning tree resulted from the chosen hypothesis from time $k - p$. We think that another interesting option would be to review a specific correlation between two different hyptheses from two different time points.
4. Taking this platform to the planning phase.

Chapter 6

Proof of Lemma 3.1

We now prove Theorem 3.1 from 3.3.3

Theorem 6.1. *The expression for $\mathbb{P}(z_{m+j} | \gamma_m = i, H_{m+j}^-)$ for any $j \in [2, p - 1]$ is given by,*

$$\mathbb{P}(z_{m+j} | \gamma_m = i, H_{m+j}^-) \approx \sum_{n=1}^S f(x_{m+j}^{n,i}, z_{m+j}) \triangleq \hat{\eta}_{m+j}^i. \quad (6.1)$$

6.1 Base Case: $j = p - 2$

We wish to prove that,

$$\mathbb{P}(z_{m+2} | \gamma_m = i, H_{m+2}^-) \approx \sum_{n=1}^S f(x_n^{m+2}, z_{m+2}). \quad (6.2)$$

Performing marginalization and chain rule yields,

$$\begin{aligned} \mathbb{P}(z_{m+2} | \gamma_m = i, H_{m+2}^-) &= \sum_{g=1}^{N_l} \int_{x_{m+2}} \mathbb{P}(z_{m+2} | l_g, x_{m+2}) \mathbb{P}(\beta_{m+2} = g | x_{m+2}) \underbrace{\mathbb{P}(x_{m+2} | \gamma_m = i, H_{m+2}^-)}_{b_m^{i-}[x_{m+2}]} dx_{m+2} = \\ &= \sum_{g=1}^{N_l} \frac{1}{|\Omega_{l_g}|} \int_{x_{m+2} \in \Omega_{l_g}} \mathbb{P}(z_{m+2} | l_g, x_{m+2}) b_m^{i-}[x_{m+2}] dx_{m+2} \end{aligned} \quad (6.3)$$

Notice argument $b_m^{i-}[x_{m+2}]$ is conditioned by H_{m+2}^- . where H_{m+2}^- includes a new obtained measurement z_{m+1} , therefore its calculation in (6.3) is not received in a direct form, as we will show in the following section.

$b_m^{i-}[x_{m+2}]$ calculation

First, let us perform marginalization over x_{m+1} and chain rule,

$$\begin{aligned} b_m^{i-}[x_{m+2}] &\equiv \mathbb{P}(x_{m+2} | \gamma_m = i, H_{m+2}^-) = \\ &= \int_{x_{m+1}} \mathbb{P}(x_{m+2} | x_{m+1}, u_{m+1}) \cdot \mathbb{P}(x_{m+1} | \gamma_m = i, H_{m+2}^-) dx_{m+1} \end{aligned} \quad (6.4)$$

Second, we take the argument $\mathbb{P}(x_{m+1} | \gamma_m = i, H_{m+2}^-)$ from (6.4), perform Bayes rules, and marginalization over all possible landmarks to obtain the measurement model,

$$\mathbb{P}(x_{m+2} | \gamma_m = i, H_{m+2}^-) = \sum_{g=1}^{N_L} \frac{1}{|\Omega_{l_g}|} \int_{x_{m+1} \in \Omega_{l_g}} \mathbb{P}(x_{m+2} | x_{m+1}, u_{m+1}) \left[\frac{\mathbb{P}(z_{m+1} | l_g, x_{m+1}) b^{i^-}[x_{m+1}]}{\mathbb{P}(z_{m+1} | \gamma_m = i, H_{m+1}^-, a_{m+1})} \right] dx_{m+1} = (6.5)$$

$$\frac{1}{\mathbb{P}(z_{m+1} | \gamma_m = i, H_{m+1}^-, a_{m+1})} \sum_{g=1}^{N_L} \frac{1}{|\Omega_{l_g}|} \int_{x_{m+1} \in \Omega_{l_g}} \mathbb{P}(x_{m+2} | x_{m+1}, u_{m+1}) \mathbb{P}(z_{m+1} | l_g, x_{m+1}) b^{i^-}[x_{m+1}] dx_{m+1}$$

$\mathbb{P}(\beta_{m+1} = g | x_{m+1})$, sets the boundaries of the integral where x_{m+1} in Ω_{l_g} . We start noticing a strong resemblance to the calculation done for $j = p - 1$. A direct approach would be to re-sample the propagated belief $b^-[x_{m+1}]$ and receive a set of samples x_{m+1}^n with $n \in [1..S]$. However, in such an approach we would need to *recalculate from scratch* the $f(x, z)$ values. In contrast we propose to re-use the previous taken samples of $b^i[x_{m+1}]$ from the previous step, and by that, *re-use* the calculated values of $f(x_{m+1}^n, z_{m+1})$. By doing so (6.5) can be denoted as,

$$b_m^{i^-}[x_{m+2}] \approx \frac{\sum_{n=1}^S \mathbb{P}(x_{m+2} | x_{m+1}^n, u_{m+1}) \cdot f(x_{m+1}^n, z_{m+1})}{\mathbb{P}(z_{m+1} | \gamma_m = i, H_{m+1}^-, a_{m+1})} \quad (6.6)$$

In the nominator we have two arguments per given sample x_{m+1}^n , the first is the motion model, and the second is the value of the f function for the given sample and measurement.

In order to calculate the denominator let us perform marginalization and chain rule over all possible landmarks and state at x_{m+1} ,

$$\mathbb{P}(z_{m+1} | \gamma_m = i, H_{m+1}^-, u_{m+1}) = \quad (6.7)$$

$$\sum_{g=1}^{N_L} \int_{x_{m+1}} \mathbb{P}(z_{m+1} | x_{m+1}, l_g) \mathbb{P}(\beta_{m+1} = g | x_{m+1}) \mathbb{P}(x_{m+1} | \gamma_m = i, H_{m+1}^-) dx_{m+1} =$$

$$\sum_{g=1}^{N_L} \frac{1}{|\Omega_{l_g}|} \int_{x_{m+1} \in \Omega_{l_g}} \mathbb{P}(z_{m+1} | x_{m+1}, l_g) b^{i^-}[x_{m+1}] dx_{m+1}$$

let us notice that the received result is identical to the result of $j = m + 1$. As before we perform reuse of the sampled values of $b^{i^-}[x_{m+1}]$ taken from the previous step, and calculated values of $f(x_{m+1}^n, z_{m+1})$, where $n \in [1..S]$. Therefore we denote,

$$\mathbb{P}(z_{m+1} | \gamma_m = i, H_{m+1}^-) \approx \sum_{n=1}^S f(x_{m+1}^n, z_{m+1}) \triangleq \eta_{m+1}^i. \quad (6.8)$$

By taking the denominator from (6.8) and placing it back in (6.6) we will get,

$$b_m^{i^-}[x_{m+2}] \approx \sum_{n=1}^S \mathbb{P}(x_{m+2} | x_{m+1}^n, u_{m+1}) \underbrace{\frac{f(x_{m+1}^n, z_{m+1})}{\eta_{m+1}^i}}_{\zeta_{m+1}^{n,i}} \quad (6.9)$$

Since the motion model in (6.9) per a given sample of x_{m+1}^n is a Gaussian distribution we can address $b^{i-}[x_{m+2}]$ as a GMM with S components, where is fact $\zeta_{m+1}^{n,i}$ is the normalized weight of a given n component.

Now that we have shown that $b_m^{i-}[x_{m+2}]$ can be addressed as a valid GMM, let us return to (6.3). In resemblance to previous step of $j = m + 1$, $\mathbb{P}(\beta_{m+2} = g \mid x_{m+2})$ sets finite boundaries to the integral, therefore in order to calculate we will sample $b_m^{i-}[x_{m+2}]$ and receive a set of samples, $x_{m+2}^n, n \in [1, S]$.

$$\mathbb{P}(z_{m+2} \mid \gamma_m = i, H_{m+2}^-) = \frac{1}{S} \cdot \sum_{n=1}^S \sum_{g=1}^{N_L} \frac{1}{|\Omega_{l_g}|} \mathbb{P}(z_{m+2} \mid l_g, x_{m+2}^n) \quad (6.10)$$

As in previous sections we can replace the landmark associated index $\beta_{m+2} = g$, with the landmark's given coordinates, l_g . For the same motivation of calculation re-use as before we can present (6.10), as

$$\mathbb{P}(z_{m+2} \mid \gamma_m = i, H_{m+2}^-) \approx \cdot \sum_{n=1}^S f(x_{m+2}^n, z_{m+2}) \triangleq \hat{\eta}_{m+2}^i \quad (6.11)$$

In conclusion we have proven that for the base case of $j = m + 2$, $\mathbb{P}(z_{m+2} \mid \gamma_m = i, H_{m+2}^-) \approx \sum_{n=1}^S f(x_{m+2}^n, z_{m+2})$.

6.2 Induction assumption

Let us make the induction assumption for $j = m + l - 1$,

$$\mathbb{P}(z_{m+j-1} \mid \gamma_m = i, H_{m+j-1}^-) \approx \sum_{n=1}^S f(x_{m+j-1}^n, z_{m+j-1}) \quad (6.12)$$

Where $x_{m+j-1}^n, n \in [1..S]$ is a set of taken samples from $\mathbb{P}(x_{m+j-1} \mid \gamma_m = i, H_{m+j-1}^-) \triangleq b_m^{i-}[x_{m+j-1}]$.

6.3 Inductive step for $j = m + l$

We wish to prove,

$$\mathbb{P}(z_{m+j} \mid \gamma_m = i, H_{m+j}^-) \approx \sum_{n=1}^S f(x_{m+j}^n, z_{m+j}) \quad (6.13)$$

We begin our induction proof by performing as before marginalization and chain rule over all given landmark index's at time $m + j$, and over the state at x_{m+j} ,

$$\mathbb{P}(z_{m+j} \mid \gamma_m = i, H_{m+j}^-) = \sum_{g=1}^{N_L} \int_{x_{m+j}} \mathbb{P}(z_{m+j} \mid l_g, x_{m+j}) \mathbb{P}(\beta_{m+j} = g \mid x_{m+j}) b_m^{i-}[x_{m+j}] dx_{m+j} \quad (6.14)$$

Where $b_m^{i-}[x_{m+j}] \doteq \mathbb{P}(x_{m+j} \mid \gamma_m = i, H_{m+j}^-)$. We notice the calculation of $b_m^{i-}[x_{m+j}]$ in (6.14), resemblance to the calculation of $b_m^{i-}[x_{m+2}]$ in (6.3). Again, in order to calculate $b_m^{i-}[x_{m+j}]$ we use chain rule and marginalization over the previous state, via x_{m+j-1} , and landmark associations, perform Bayes rule to subtract the observation model for measurement z_{m+j-1} ,

$$b_m^{i-}[x_{m+j}] = \int_{x_{m+j-1}} \mathbb{P}(x_{m+j} \mid x_{m+j-1}, u_{m+j-1}) \cdot \frac{[\sum_{g=1}^{N_L} \mathbb{P}(z_{m+j-1} \mid x_{m+j-1}, l_g) \cdot \mathbb{P}(\beta_{m+j-1} = g \mid x_{m+j-1}) \cdot b_m^{i-}[x_{m+j-1}]] dx_{m+j-1}}{\mathbb{P}(z_{m+j-1} \mid \gamma_m = i, H_{m+j-1}^-)} \quad (6.15)$$

In order to calculate $b_m^{i-}[x_{m+j-1}]$ at (6.15) in the naive approach one needs to marginalize and perform Byes rule till retrieving the calculations to the time of the hypothesis we wish to reevaluate its weight. Instead let us look on the argument inside the brackets in (6.15), and see it resembles the value of $\mathbb{P}(z_{m+j-1} \mid \gamma_m = i, H_{m+j-1}^-)$ from our induction assumption in 6.2. So instead of the direct approach that requires recalculation and re-sample of $b_m^{i-}[x_{m+j-1}]$, we will re-use the set of samples x_{m+j-1}^n , and by that the set of calculated values of the f function from the induction assumption. So (6.15) can appear as such,

$$b_m^{i-}[x_{m+j}] \approx \sum_{n=1}^S \mathbb{P}(x_{m+j} \mid x_n^{m+j-1}, u_{m+j-1}) \cdot \frac{f(x_{m+j-1}^n, z_{m+j-1})}{\mathbb{P}(z_{m+j-1} \mid \gamma_m = i, H_{m+j-1}^-)} \quad (6.16)$$

For the denominator in resemble to 6.1 we marginalize over all given landmarks and x_{m+j-1} , and perform chain rule as before,

$$\begin{aligned} \mathbb{P}(z_{m+j-1} \mid \gamma_m = i, H_{m+j-1}^-) &= \sum_{j=1}^{N_L} \frac{1}{|\Omega_{l_g}|} \int_{x_{m+j-1} \in \Omega_{l_g}} \mathbb{P}(z_{m+j-1} \mid l_g, x_{m+j-1}) b_m^{i-}[x_{m+j-1}] dx_{m+j-1} \\ &\approx \frac{1}{|\Omega_{l_g}|} \sum_{n=1}^S \mathbb{P}(z_{m+j-1} \mid l_g, x_{m+j-1}^n) \doteq \hat{\eta}_{m+j-1}^i \end{aligned} \quad (6.17)$$

By placing (6.17) into (6.16) we get,

$$b_m^{i-}[x_{m+j}] \approx \sum_{n=1}^S \mathbb{P}(x_{m+j} | x_n^{m+j-1}, u_{m+j-1}) \cdot \underbrace{\frac{f(x_{m+j-1}^n, z_{m+j-1})}{\eta_{m+j-1}^i}}_{\zeta_{m+j-1}^{n,i}} \quad (6.18)$$

In resemble to (6.9), in (6.18) we get a GMM with S components, where $\mathbb{P}(x_{m+j} | x_n^{m+j-1}, u_{m+j-1})$ is a motion model with Gaussian distribution per a given sample, x_{m+j-1}^n , and $\zeta_{m+j-1}^{n,i}$ acts as the normalized weight for a given n hypothesis in the GMM.

Now after we have shown that $b_m^{i-}[x_{m+j}]$ is a valid GMM, we can take a set of samples x_{m+j}^n where $n \in [1..S]$. And by that (6.14) yields into,

$$\mathbb{P}(z_{m+j} | \gamma_m = i, H_{m+j}^-) \approx \frac{1}{S} \sum_{n=1}^S \sum_{g=1}^{N_L} \frac{1}{|\Omega_{l_g}|} \mathbb{P}(z_{m+j} | l_g, x_{m+j}^n) \doteq \sum_{n=1}^S f(x_{m+j}^n, z_{m+j}), \quad (6.19)$$

where (6.19) is what we wished to prove by induction.

Bibliography

- [1] O. Shelly and V. Indelman, “Hypotheses disambiguation in retrospective,” *IEEE Robotics and Automation Letters (RA-L)*, 2022, accepted.
- [2] C. Cadena, L. Carlone, H. Carrillo, Y. Latif, D. Scaramuzza, J. Neira, I. D. Reid, and J. J. Leonard, “Simultaneous localization and mapping: Present, future, and the robust-perception age,” *IEEE Trans. Robotics*, vol. 32, no. 6, pp. 1309 – 1332, 2016.
- [3] R. Smith and P. Cheeseman, “On the representation and estimation of spatial uncertainty,” *Intl. J. of Robotics Research*, vol. 5, no. 4, pp. 56–68, 1987.
- [4] H. Durrant-Whyte, “Uncertain geometry in robotics,” *IEEE Trans. Robot. Automat.*, vol. 4, no. 1, pp. 23–31, 1988.
- [5] T. Bailey and H. Durrant-Whyte, “Simultaneous localisation and mapping (SLAM): Part II state of the art,” *Robotics & Automation Magazine*, Sep 2006.
- [6] A. Davison, I. Reid, N. Molton, and O. Stasse, “MonoSLAM: Real-time single camera SLAM,” *IEEE Trans. Pattern Anal. Machine Intell.*, vol. 29, no. 6, pp. 1052–1067, Jun 2007.
- [7] F. Dellaert and M. Kaess, “Square Root SAM: Simultaneous localization and mapping via square root information smoothing,” *Intl. J. of Robotics Research*, vol. 25, no. 12, pp. 1181–1203, Dec 2006.
- [8] J. Folkesson and H. Christensen, “Graphical SLAM – a self-correcting map,” in *IEEE Intl. Conf. on Robotics and Automation (ICRA)*, vol. 1, 2004, pp. 383–390.
- [9] G. Grisetti, C. Stachniss, S. Grzonka, and W. Burgard, “A tree parameterization for efficiently computing maximum likelihood maps using gradient descent,” in *Robotics: Science and Systems (RSS)*, Jun 2007.
- [10] M. Kaess, H. Johannsson, R. Roberts, V. Ila, J. Leonard, and F. Dellaert, “iSAM2: Incremental smoothing and mapping using the Bayes tree,” *Intl. J. of Robotics Research*, vol. 31, no. 2, pp. 217–236, Feb 2012.
- [11] M. Kaess, A. Ranganathan, and F. Dellaert, “iSAM: Incremental smoothing and mapping,” *IEEE Trans. Robotics*, vol. 24, no. 6, pp. 1365–1378, Dec 2008.

- [12] R. Kümmerle, G. Grisetti, H. Strasdat, K. Konolige, and W. Burgard, “g2o: A general framework for graph optimization,” in *Proc. of the IEEE Int. Conf. on Robotics and Automation (ICRA)*, Shanghai, China, May 2011.
- [13] F. Dellaert, “Factor graphs and GTSAM: A hands-on introduction,” Georgia Institute of Technology, Tech. Rep. GT-RIM-CP&R-2012-002, September 2012.
- [14] S. Agarwal, K. Mierle, and Others, “Ceres solver,” Google, Tech. Rep., 2016, <http://ceres-solver.org>.
- [15] S. Pathak, A. Thomas, A. Feniger, and V. Indelman, “Da-bsp: Towards data association aware belief space planning for robust active perception,” in *Eur. Conf. on AI (ECAI)*, September 2016.
- [16] S. Pathak, A. Thomas, and V. Indelman, “A unified framework for data association aware robust belief space planning and perception,” *Intl. J. of Robotics Research*, vol. 32, no. 2-3, pp. 287–315, 2018.
- [17] V. Tchuiev, Y. Feldman, and V. Indelman, “Data association aware semantic mapping and localization via a viewpoint-dependent classifier model,” in *IEEE/RSJ Intl. Conf. on Intelligent Robots and Systems (IROS)*, 2019.
- [18] M. Hsiao and M. Kaess, “Mh-isam2: Multi-hypothesis isam using bayes tree and hypo-tree,” in *IEEE Intl. Conf. on Robotics and Automation (ICRA)*, May 2019.
- [19] T. Fortmann, Y. Bar-Shalom, and M. Scheffe, “Multi-target tracking using joint probabilistic data association,” in *Proc. 19th IEEE Conf. on Decision & Control*, 1980.
- [20] V. Indelman, E. Nelson, J. Dong, N. Michael, and F. Dellaert, “Incremental distributed inference from arbitrary poses and unknown data association: Using collaborating robots to establish a common reference,” *IEEE Control Systems Magazine (CSM), Special Issue on Distributed Control and Estimation for Robotic Vehicle Networks*, vol. 36, no. 2, pp. 41–74, 2016.
- [21] G. H. Lee, F. Fraundorfer, and M. Pollefeys, “Robust pose-graph loop-closures with expectation-maximization,” in *IEEE/RSJ Intl. Conf. on Intelligent Robots and Systems (IROS)*, 2013, pp. 556–563.
- [22] N. Sünderhauf and P. Protzel, “Switchable constraints for robust pose graph SLAM,” in *IEEE/RSJ Intl. Conf. on Intelligent Robots and Systems (IROS)*, 2012.
- [23] C. Stachniss, D. Haehnel, and W. Burgard, “Exploration with active loop-closing for FastSLAM,” in *IEEE/RSJ Intl. Conf. on Intelligent Robots and Systems (IROS)*, 2004.

- [24] L. Carlone, A. Censi, and F. Dellaert, “Selecting good measurements via l1 relaxation: A convex approach for robust estimation over graphs,” in *IEEE/RSJ Intl. Conf. on Intelligent Robots and Systems (IROS)*. IEEE, 2014, pp. 2667–2674.
- [25] E. Olson and P. Agarwal, “Inference on networks of mixtures for robust robot mapping,” *Intl. J. of Robotics Research*, vol. 32, no. 7, pp. 826–840, 2013.
- [26] L. Wong, L. P. Kaelbling, and T. Lozano-Pérez, “Data association for semantic world modeling from partial views,” in *International Symposium for Robotics Research*. Intl. Foundation of Robotics Research, 2013.
- [27] H. Yang, P. Antonante, V. Tzoumas, and L. Carlone, “Graduated non-convexity for robust spatial perception: From non-minimal solvers to global outlier rejection,” *IEEE Robotics and Automation Letters*, vol. 5, no. 2, pp. 1127–1134, 2020.
- [28] P. Antonante, V. Tzoumas, H. Yang, and L. Carlone, “Outlier-robust estimation: Hardness, minimally-tuned algorithms, and applications,” *arXiv preprint arXiv:2007.15109*, 2020.
- [29] D. Fourie, J. Leonard, and M. Kaess, “A nonparametric belief solution to the bayes tree,” in *IEEE/RSJ Intl. Conf. on Intelligent Robots and Systems (IROS)*, 2016.
- [30] N. Atanasov, B. Sankaran, J. Ny, G. J. Pappas, and K. Daniilidis, “Nonmyopic view planning for active object classification and pose estimation,” *IEEE Trans. Robotics*, vol. 30, pp. 1078–1090, 2014.
- [31] S. M. Chaves, J. M. Walls, E. Galceran, and R. M. Eustice, “Risk aversion in belief-space planning under measurement acquisition uncertainty,” in *IEEE/RSJ Intl. Conf. on Intelligent Robots and Systems (IROS)*. IEEE, 2015, pp. 2079–2086.
- [32] T. Patten, M. Zillich, R. Fitch, M. Vincze, and S. Sukkariéh, “Viewpoint evaluation for online 3-d active object classification,” *IEEE Robotics and Automation Letters (RA-L)*, vol. 1, no. 1, pp. 73–81, January 2016.
- [33] B. Sankaran, J. Bohg, N. Ratliff, and S. Schaal, “Policy learning with hypothesis based local action selection,” *arXiv preprint arXiv:1503.06375*, 2015.
- [34] S. Agarwal, A. Tamjidi, and S. Chakravorty, “Motion planning in non-gaussian belief spaces for mobile robots,” *arXiv preprint arXiv:1511.04634*, 2015.
- [35] N. J. Gordon, D. J. Salmond, and A. F. Smith, “Novel approach to nonlinear/non-gaussian bayesian state estimation,” in *IEE proceedings F (radar and signal processing)*, vol. 140, no. 2. IET, 1993, pp. 107–113.

בעבודה זו כפי שנאמר אנו מניחים כי מודל שיוך המידע אינו מושלם, כיוצא מכך בניגוד לדעה הרווחת בו מניחים כי החישה מתבצעת רק בקורולציה עם אוביקט אחד, בעבודה זו אנו לוקחים בחשבון כי שיוך המידע של המדידה הנוכחית יכול להיות עם סט של אוביקטים. על כן האמונה שלנו בנק' זמן מסויימת מתפצלת למס' אמונות החיות במקביל, כאשר כל אחת מהן הינה פונקציית הסתברות בעלת פילוג גאוס, ויחדיו Gaussian Mixture Model (GMM). למעשה כל היפותזה בסכום הכולל של GMM מוכפלת בהסתברות שלה להיות ההיפותזה בעלת שיוך המידע ה"נכון", לאיבר זה אנו קוראים משקל (weight), כאשר כתוצאה כ-marginalization, סך המשקלים הינו אחד.

אנו עוסקים במקרה הפסיבי בו ה GMM בנק' זמן הסופית נתון ומוגמר, וכעת עלינו לבצע הערכה מחדש של המשקל של היפותזות מפתח כלשהי מהעבר. בחישוב המלא אנו מציגים כי המשקל המעודכן הינו תוצאה של המשקל המקורי מוכפל בגורם עידכון, גורם זה הינו מכפלה של איברים כאשר כל איבר הינו עידכון הנובע מנק' הזמן הרלוונטית בין הזמן של היפותזות המפתח לזמן הנוכחי. בגישה שלנו אנו מציגים גישה אינקרמנטלית, שבה חישוב של כל איבר שכזה בצעד מסויים מתבססת על החישובים שנעשו בצעד שקודם אליו. יכולת זו של שימוש חוזר בחישובים מקטינה את זמן הריצה לעומת הגישה של חישוב מחדש בסדר גודל.

בסימולציות שבוצעו נלקחו בחשבון סביבות בעלות דו משמעויות רבות, בהן מספר רב של איברים זהים שהיו מפוזרים במרחב. הסימולציות בוצעו בשני חלקים עיקרים. הראשון חישוב של ה GMM הסופי בתרחישים של בין חמישה לעשרה צעדים, והשני חישוב מחדש של פיזור המשקולות צעד אחד קדימה מנק' ההתחלה של הרובוט. בשתי הדוגמאות המוצגות בעבודה זו אנו יכולים לראות כי על פי פיזור המשקולות בנק' המפתח בזמן המקורי לא היה ניתן לבצע שיוך מדידה מלא, ועם זאת כן בהינתן המידע עד סוף המסלול.

בנוסף על כך אנו משווים את זמני הריצה השונים של הגישה הנאיבית המבצעת חישוב חדש לכל איבר, וגם של הגישה של שימוש חוזר בחישובים מהצעד קודם שאנו מציגים, כאשר גרף אחד הינו כפונקציה של המרחק בין הזמן הנוכחי לנק' המפתח, וגרף שני כפונקציה של מס' הדגימות. שני הגרפים מראים יתרון ברור לגישה שאנו מציגים.

נוסף על כך ביצענו סימולציות המראות את היכולת לבצע גיזום (pruning) באופן כללי יותר מהיום, כאשר אנו משליכים את היכולת שלנו לבצע גיזום של היפותזות עבר על כל עץ ההיפותזות הנובעות ממנה, וזאת בדגש על אלו בזמן הנוכחי. לדבר יש מספר השפעות מעניינות, הן בצמצום מספר ההיפותזות הכוללות לאורך כל המסלול של הרובוט, והן מבחינת פיזור המשקולות בזמן הסופי כתוצאה מנירמול מספר מצומצם יותר של המשקולות.

לסיכום אנו מאמינים כי עבודה זו מראה כי איבחון מחדש של היפותזות עבר בהינתן מידע חדש יכול לסייע בחישה יותר חסינה לסביבות בעלות דו משמעות. גישה זו יכולה להילקח לכל מיני כיוונים, כמו ביצוע סימולציית בסביבה אמיתית בעלת דו משמעות, הורדת ההנחה שהמפה ידועה מראש, ולבסוף באופן קבלת ההחלטות של הרובוט בשלב התכנון.

תקציר

ניווט אוטונומי בסביבות לא ידועות הוא חלק חיוני במספר תחומים ברובוטיקה. במהלך המסלול של הרובוט קיימת אי וודאות באיכון המיקום של הרובוט, דבר אשר יכול לנבוע מאי וודאות הן בתנועת הרובוט והן בחישה עצמה. יש לציין כי בנוסף לכך המיקום הראשוני של הרובוט גם הוא אינו ידוע באופן מוחלט (נקרא "prior"). על מנת שנוכל לבצע שיערוך של מיקום הרובוט אנו מייצרים ווקטור של נעלמים המתאר את מיקום הרובוט לאורך המסלול. באופן כללי כאשר המרחב בו אנו נמצאים אינו וודאי גם כן, ווקטור המצב יכול לתוכו גם תת ווקטור המתאר את מיקום האובייקטים השונים במרחב. משערך זה אשר נבנה על ידי פונקציית הסתברות הידועה גם בשם אמונה (belief).

אחד המרכיבים החיוניים הן בתהליך ההסקה והן בתהליך החישה הינו תהליך שיוך המידע (Data association), כלומר בעת קבלת מדידה, על הרובוט לבצע שיוך של המדידה הנוכחית אל האובייקט הנכון במרחב ממנו היא התקבלה. אם זאת בעולם האמיתי במספר רב של תרחישים קיימת דו משמעויות - למשל מספר רב של כיסאות או שולחנות זהים המפוזרים במרחב, דבר זה גורם לחישה (perception) להיות יותר מתאגרת ופחות חסינה. יש לציין כי בעיית שיוך המידע אינה מסתכמת אך ורק באובייקטים דומים, היא יכולה לנבוע גם עקב מגבלת המרחק של חיישני המדידה.

נשאלת השאלה מה עלול לקרות עקב שיוך מידע לא נכון. אובכן בצורה הפשוטה דבר זה יכול לגרום לסטייה מסויימת מהמסלול האופטימלי של הרובוט, ולהגדלת אי הוודאות הקיימת במרחב לפרק זמן מסויים. עם זאת במקרים מסויימים דבר זה עלול אף לגרום לתוצאות הרסניות - למשל הגעת הרובוט למבוי סתום, ועל כן יש חשיבות רבה לקחת זאת בחשבון בעת פיתוח גישות להסקה חסינה במרחב הסתברותי.

עד כה בקהילת המחקר ברובוטיקה התעסקו בפיתוח גישות אלו, כאשר הרוב התעסקו בתחום ההסקה, וחלק קטן באופן המשפיע על בחירת סט הפעולות שנלקחות על ידי הרובוט ("תכנון"). העבודות השונות התמקדו הן בפיתוח מודלים גרפים מעודכנים הלוקחים בחשבון את אי הוודאות הקיימת במרחב, מציאת דרכי עידכון אינקרמטליות על מנת לצמצם בזמני חישוב, ובמקרה האקטיבי, מציאת פעולה המקטינה את אי הוודאות המצטברת של ההיפותזות השונות בזמן מסויים. עם זאת יש לציין כי כל המחקרים המצויינים לעיל התעסקו בפיתוח גישות הסקה אשר מתעסקות בנקי זמן הנוכחית או העתידית במקרה של תכנון, אף אחת מהן לא שקלה את ההשפעה שיכולה להיות למידע שנאסף עד נקי הזמן הנוכחית, על אי וודאות מסויימת מנקי זמן עבר במסלולו של הרובוט.

עבודה זו מציעה גישה של עדכון היפותזות בדיעבד. כלומר לאחר שכל המידע נאסף עד נקי הזמן הנוכחית, אנו יכולים לבצע הערכה מחדש של נכונות היפותזות מפתח כלשהי מהעבר. כאשר על מנת לעשות זאת אנו לוקחים בחשבון את כל האי וודאויות שנאספו עד נקי הזמן הנוכחית. מוטיבציה לכך יכולה להינתן במקרה הפשוט שבו לאור המידע הקיים עד לנקודת המפתח לא יכולנו לבצע שיוך מידע נכון, עם זאת כאשר לוקחים בחשבון מידע שנאסף עד סוף המסלול של הרובוט דבר זה הינו בר ביצוע.

בנוסף לכך אנו מראים בעבודה זו איך לעדכון היפותזות עבר כלשהי יכולות להיות השלכות גם על הערכה של שיוך מידע ספציפי, ובנוסף על היכולת שלנו לגזום (pruning) את הצאצאים של היפותזות המפתח במקרה שבו החישוב מחדש מאפשר זאת

המחקר נעשה בהנחיית פרופסור ואדים אינדלמן בתכנית הטכניונית למערכות אוטונומיות.

תודות

אני מודה לטכניון על התמיכה הכספית הנדיבה בהשתלמותי

עדכון היפותזות בדיעבד עבור חישה חסינה בסביבות עם דו-משמעות

חיבור על מחקר

לשם מילוי חלקי של הדרישות לקבלת התואר מגיסטר
למדעים במערכות אוטונומיות ורובוטיקה

אוהד שלי

הוגש לסנט הטכניון - מכון טכנולוגי לישראל
אדר א' תשפ"ב, חיפה, פברואר 2022

**עדכון היפותזות בדיעבד עבור חישה
חסינה בסביבות עם דו-משמעות**

אוהד שלי